CHAPTER 1: LITERATURE REVIEW

1.1. INTRODUCTION

Since the discovery of viruses as 'filterable disease agents', approximately 110 years ago, the field has expanded enormously with viruses continually being discovered in many different species. The currently identified and characterised viruses probably represent only a fraction of the viral diversity, or virosphere, predicted to be present in the biosphere. Suttle (2005) proposes that viruses are the most abundant biological entities on the planet and are, in terms of biomass, second only to prokaryotes. These recent insights imply that, in most cases, excessive virulence in viruses is an exception, and probably an evolutionary dead-end strategy. It is, nonetheless, these virulent viruses that have received most of our attention because of their devastating disease causing capabilities. Remarkable progress has been made in our understanding of exactly how these viruses cause disease, the myriad strategies they use to multiply within their hosts, the subtle and often surprising interactions that exist between them and their hosts, and the diverse tactics they employ to evade detection and eradication by their hosts' defence systems.

The focus of this investigation is a virus that causes one of the most lethal viral diseases of equids, African horsesickness (AHS). This review will summarise the progress that has been made in research on African horsesickness virus (AHSV), and will highlight the need for further investigation into the viral factors that contribute to the molecular basis of AHS disease and pathogenesis. The emphasis of this review will be on the non-structural AHSV protein NS3 that has been implicated by previous studies to be a potentially important factor in disease pathogenesis and virulence. Viral proteins that share similar structural and/or functional characteristics to AHSV NS3 will also be discussed.

1.2. AFRICAN HORSESICKNESS (AHS)

1.2.1. History and current status of AHS

Although the first known historical report of a disease resembling AHS was in Yemen in 1327, the disease almost certainly originated in Africa (Coetzer & Guthrie, 2004). Here it was probably first recognised following the introduction of horses into central and east Africa. In southern Africa, were AHS is endemic today, the first serious outbreak occurred in 1719 when over 1 700 horses died. Over the subsequent years at least 10 major and numerous lesser outbreaks have been recorded in this region. The most severe outbreak occurred in South Africa in 1854 causing the death of over 70 000 horses. The incidence, range and severity of outbreaks in this region has decreased greatly over the past century probably relating to the decline in horse and zebra

numbers, and the introduction of AHS vaccines. The disease has made incursions into other areas including the Middle East, Arabia, India and Pakistan between 1959 and 1961, North Africa and Spain from 1955 to 1956, and Spain, Portugal and Morocco in 1987 to 1991 (Mellor & Hamblin, 2004).

The pioneering work on AHS and the discovery of the etiological agent, African horsesickness virus (AHSV), occurred in the early 1900s. M'Fadyean showed that AHS was transmissible through filtered bacteria-free blood from an infected horse, his results were confirmed and expanded on by Sir Arnold Theiler in 1901. Theiler commenced research on AHSV, demonstrating the plurality of the virus strains and their impact on vaccination, as well as describing the disease forms of AHS (Theiler, 1921). In the late 1960s Dr Verwoerd at the Onderstepoort Veterinary Research Institute showed that AHSV had a segmented double stranded RNA (dsRNA) genome. Since this early work research into AHSV, and other related dsRNA viruses, has expanded greatly and will be outlined later in this review.

Currently there is no specific treatment available for AHS. Animals that recover from infections show life-long immunity to the serotype they were infected with and partial immunity to similar serotypes (Erasmus, 1998). Prevention and control measures include the restriction of animal movement, slaughter of viraemic animals, stabling susceptible horses at the times at which the vector is most active (at twilight and during the night), vector control (insecticides and repellents) and vaccination (Mellor & Hamblin, 2004). The only widely available commercial AHSV vaccines are supplied by Onderstepoort Biological Products, Onderstepoort, South Africa (www.obpvaccines.co.za). These vaccines are polyvalent attenuated cell culture adapted viruses. Adult horses in southern Africa, excluding regions of the Western Cape province, are vaccinated annually in spring in an attempt to prevent disease and control outbreaks (Coetzer & Guthrie, 2004). Monovalent vaccines are sometimes additionally administered during outbreaks. Concerns over the safety and efficacy of these vaccines have been raised following cases of alleged vaccine failure and vaccine-induced disease. Analysis of AHSV isolates from three post-vaccination horses that died or exhibited AHS symptoms, revealed reassortment of the vaccine but reassortants were found not to be pathogenic or lethal when administered to susceptible horses (Von Teichman & Smit, 2008). Further large scale studies would however have to be conducted to determine the frequency of vaccine reassortment, and the potential association of the vaccine with AHS disease and AHS-induced death.

During AHS outbreaks, or potential outbreaks, the detection and serotyping of AHSV is crucial and should occur timeously. Although the clinical signs and lesions typical of AHS are specific they can be confused with other diseases. Rapid serotyping is also essential for the selection of

the correct vaccine serotype for efficient control of the spread of the disease, particularly when the outbreak occurs in a non-endemic area (Koekemoer *et al.*, 2000). Several techniques have therefore been tailored for the detection of the AHSV RNA segments, antigens and antibodies. These include, for example, a novel real time PCR assay developed for the detection and serotyping of AHSV within two to three hours (Rodriguez-Sanchez *et al.*, 2008).

1.2.2. Host range and transmission

Many species of vertebrate are susceptible to AHSV infection, including zebras, horses, mules, donkeys, dogs, camels and elephants. Signs of clinical infection are rarely seen in zebras and they have long been considered to be the natural vertebrate host and reservoir of AHSV. They are believed to play a vital role in the persistence of the virus in Africa. The introduction of zebras, with sub-clinical infection, into a safari park close to Madrid is the likely cause of the outbreak of AHS in Spain in 1987. Horses, mules and donkeys are not considered long-term reservoirs, involved in the permanent persistence of the virus, because of the high mortality rate frequently recorded, particularly in horses (Mellor & Hamblin, 2004).

AHS is not contagious, and the virus is transmitted by *Culicoides* biting midges of which the most important vectors in Africa are *C. imicola* and *C. bolitinos* (Venter *et al.,* 2000). The insect is most active during the summer, when the optimal conditions of warm weather, high rainfall and wind occur. *Culicoides imicola* breeds in wet soil and in years of heavy rain its population can increase over 200-fold (Meiswinkel, 1998). The spread of the virus has been limited by the climatic conditions favoured by these insects (Meiswinkel, 1998; Mellor *et al.*, 1998). *Culicoides imicola* is common throughout Africa and south east Asia, and is now known to be widespread across the southern parts of Europe (Mellor & Hamblin, 2004). Climate change however may increase the vector range and so doing raise the possibility of the international spread of AHS (Purse *et al.*, 2005; Gould & Higgs, 2009).

1.2.3. AHS disease forms and pathogenesis

African horsesickness has four clinicopathological forms: horsesickness fever, cardiac form, pulmonary form and mixed form. Horsesickness fever is characterised by a remittent mild to moderate fever and is often subclinical with no associated mortality. It occurs frequently following infection with less virulent strains of virus or when some degree of immunity exists (for example horses that have been vaccinated with or exposed to a heterologous serotype). This is the only form of disease exhibited by zebra. The cardiac (sub-acute) form is characterised by fever (lasting 3-6 days), subcutaneous oedema of the head, neck and chest and supraorbital fossa, and

haemorrhages of the eyes and ventral tongue surface. Death is as a result of cardiac failure. Mortality rates with this form range from 50 to 60%. The pulmonary (peracute) form develops rapidly (1 to 3 days), with marked depression, fever, increased respiratory rate, severely laboured breathing, profuse sweating and coughing spasms. A frothy, serofibrinous fluid may exude from the nostrils. The mortality rate in horses with this form is high, exceeding 95%, and death is due to a lack of oxygen. The mixed form of AHS is the most common and is a combination of the cardiac and pulmonary forms with mortality rates between 50 and 90% (Coetzer & Guthrie, 2004; Mellor & Hamblin, 2004).

The form of disease in infected horses may be the result of a variety of factors, including the route of infection, tropism of sub-populations of virus particles, host immune status, permissivity and genetic susceptibility (Laegreid *et al.*, 1993). However, the principal determinant of the clinical form of the disease was shown in experimentally infected naive horses to be the viral virulence phenotype (Laegreid *et al.*, 1993).

The clinical and molecular basis of AHS pathogenesis is not well understood. The key pathological features of AHS are oedema, effusion and haemorrhage, and the clinical signs are thought to develop as a result of damage to the circulatory and respiratory systems (Mellor & Hamblin, 2004). On infection of the vertebrate host initial virus multiplication occurs in local lymph nodes and the virus is then spread throughout the body via the circulatory system. This primary viraemia enables the virus to infect target organs; namely the lungs, spleen, other tissues of the lymphoid system, and various endothelial cells (EC). Replication of the virus in these tissues then leads to secondary viraemia that usually coincides with the onset of fever (Mellor & Hamblin, 2004). In experimentally infected horses, with the peracute form of disease, viral antigen is found mainly in the cardio-vascular and lymphatic systems. In these horses AHSV antigen was located primarily in EC of capillaries, and small venous and arteriolar vessels, particularly of cardiopulmonary tissues suggesting that EC are the main target of AHSV infection during the late stages of this form of the disease (Wohlsein *et al.*, 1997). AHSV has been shown to infect pulmonary microvascular EC, causing pronounced cell swelling, discontinuity of the plasma membrane and loss of structural detail in severely affected cells (Laegreid *et al.*, 1992a). Skowneck *et al.* (1995) suggest that it is the loss of the EC barrier function that results in the development of the prominent pathological features. Damage to EC and loss of integrity of intercellular junctions could result in loss of EC barrier function and the subsequent development of oedema (Laegreid *et al.*, 1992a; Skowronek *et al.*, 1995; Gomez-Villamandos *et al.*, 1999). Virulence variants of AHSV have also been shown to differ in their ability to infect and damage cultured EC (Laegreid *et al.*, 1992b).

1.3. AFRICAN HORSESICKNESS VIRUS (AHSV)

1.3.1. Classification

AHSV is a member of the genus *Orbivirus* in the family *Reoviridae*. Members of the *Orbivirus* genus frequently have similar morphological and molecular characteristics but distinct host ranges and pathobiological properties (Roy, 1996). The prototype orbivirus, bluetongue virus (BTV), is similar in molecular constitution and morphology to AHSV but causes disease in cattle and sheep (Mellor & Hamblin, 2004). Another closely related orbivirus, equine encephalosis virus (EEV), infects equids but disease is subclinical (Coetzer & Erasmus, 1994). Biting midges (*Culicoides* spp.) are the principal vectors for all three of these orbiviruses.

Nine serotypes of AHSV have been identified that are antigenically distinct based on neutralisation studies of the major outer capsid viral protein VP2 (Howell, 1962).

1.3.2. Genome

Orbiviruses are characterised by a genome consisting of 10 double-stranded (ds) RNA segments of different sizes encoding at least seven structural (VP1-VP7) and four non-structural proteins, NS1, NS2, NS3 and NS3A (Bremer, 1976; Huismans, 1979; Mertens *et al.*, 1984; Mertens, 2004). The dsRNA genome segments are enclosed within the inner core of the virus and are never exposed in the cytoplasm (Mertens & Diprose, 2004). The total AHSV genome is approximately 18 kilobase pairs (kb) in length. The 5' non-coding regions of the genome segments are 12 to 35 base pairs (bp) in length and the 3' non-coding regions 29 to 100 bp. Partial inverted complementarity is observed between the 5' and 3' end sequences within each AHSV segment, indicating the potential for the formation of secondary structure in the single stranded (ss) RNA forms (Roy *et al.*, 1994).

1.3.3. Structural proteins

The mature AHSV virion is a non-enveloped icosahedral particle composed of two distinct layers; a core or inner capsid surrounded by an outer capsid (Roy *et al.*, 1994).

1.3.3.1. Outer capsid proteins

The outer capsid of AHSV is composed of structural proteins VP2 and VP5. VP2 (encoded by segment 2) is the major component of the outer shell of the virus particle and is involved in virus-

cell attachment and penetration (Roy *et al.*, 1994). The full-length VP2 genes of all nine AHSV serotypes have been cloned, expressed and the protein sequences aligned. Sequence homology varied between 47.6 and 71.4 % indicating that VP2 is the most variable AHSV protein (Potgieter *et al.*, 2003). The major serotype-specific neutralising epitopes of AHSV are located on VP2 (Burrage *et al.*, 1993; Martinez-Torrecuadrada *et al.*, 1994; Martinez-Torrecuadrada & Casal, 1995; Bentley *et al.*, 2000; Martinez-Torrecuadrada *et al.*, 2001). Recombinant baculovirus expressed VP2, alone or in combination with VP5 and/or VP7, provided full protection against AHSV challenge in horses (Martinez-Torrecuadrada *et al.*, 1996; Roy *et al.*, 1996; Stone-Marschat *et al.*, 1996). The insolubility and aggregation of the protein have however made the development of VP2 subunit vaccines problematic (Du Plessis *et al.*, 1998). AHSV serotype 4 VP2 and VP5 have successfully been expressed from individual alphavirus-based vaccine vectors, initial tests however failed to induce a neutralising antibody response in horses (MacLachlan *et al.*, 2007).

AHSV VP5 is encoded by segment 6 and its biological function remains unknown, although it is probably analogous to that of its BTV counterpart (Martinez-Torrecuadrada *et al.*, 1999). In BTV, VP5 is believed to play an important role during cell entry. Following attachment to the membrane the virus enters the cell via the clathrin-dependant endocytic pathway. The virus is then internalised into early endosomes where separation of the outer and inner capsid layers is induced by low pH (Forzan *et al.*, 2007). The transcriptionally active core is then delivered into the cell cytoplasm. Purified BTV VP5 was shown to permeabilise both mammalian and *Culicoides* cell membranes (Hassan *et al.*, 2001) and to act as a fusion protein, at low pH, when fused to a transmembrane anchor and expressed on the cell surface (Forzan *et al.*, 2004). Both permeabilisation and fusion activities are mediated by two N-terminal amphipathic helixes. BTV VP5 is believed therefore to play a major role in destabilising the membrane of the endocytosed vesicle allowing the release of the viral core into the cytoplasm (Hassan *et al.*, 2001; Forzan *et al.*, 2004). AHSV VP5 contains similar amphipathic helix motifs and appears to be cytotoxic when expressed in insect cells (Roy *et al.*, 1994).

1.3.3.2. Inner capsid proteins

The genome of AHSV is encapsidated by an inner core particle composed of two major structural proteins (VP7 and VP3) and three core-associated enzymes (VP1, VP4 and VP6). The genome remains within the inner core throughout the replication cycle (Mertens & Diprose, 2004). This is essential as direct contact between the dsRNA and the host cell cytoplasm would activate an array of host antiviral mechanisms and degradation by nucleases. In BTV the core particle has been studied to atomic resolution by X-ray crystallography, revealing important information with

regard to the organisation of VP3 and VP7, the packaging of the genome within the core, as well as how the simultaneous and repeated transcription of all 10 genome segments occurs within the confined interior of the core (Grimes *et al.*, 1998; Mertens & Diprose, 2004).

VP3 and VP7 (encoded by segments 3 and 7 respectively) are highly conserved between members of the O*rbivirus* genus and contain the group-specific antigenic determinants (Roy, 1996). When AHSV VP3 and VP7 were co-expressed in insect cells they aggregated to form empty core-like particles (CLP) (Maree *et al.*, 1998). When expressed alone in insect cells AHSV VP7 forms hexagonal crystalline structures due to its insoluble and hydrophobic nature (Chuma *et al.*, 1992).

VP1 and VP4 (encoded by segment 1 and 4 respectively) are considered to have replicase-transcriptase and guanyl transferase activity respectively, analogous to BTV VP1 and VP4 (Roy *et al.*, 1994). VP6 (encoded by segment 9) is believed to act as the viral helicase catalysing the unwinding of the dsRNA segments prior to transcription. The protein shares a degree of sequence similarity to an *E. coli* helicase (Turnbull *et al.*, 1996) and has the ability to bind both single-stranded (ss) and ds RNA and DNA (De Waal & Huismans, 2005). A recent study revealed the potential for a second open reading frame (ORF) on genome segment 9 (Firth, 2008), whether this ORF is expressed, and what functional role the encoded protein may play, remains to be experimentally investigated. VP1, VP4 and VP6 therefore provide the enzymatic machinery needed to convert dsRNA into a translatable mRNA, as well as synthesizing a negative RNA strand from a positive RNA template to reform the dsRNA genome segments in progeny virus cores.

1.3.4. Non-structural proteins

AHSV NS1 is encoded by segment 5. NS1 is highly conserved; a comparison of NS1 sequences from AHSV serotypes 4, 6 and 9 revealed 95 to 98% amino acid homology (Maree & Huismans, 1997). The protein is synthesised in large amounts (up to 25% of the total viral proteins in BTV-infected cells) and forms the characteristic tubules that are observed in orbiviral infected cells throughout the infection cycle (Huismans & Els, 1979). NS1 contains several conserved cysteine residues that are believed to be of functional significance in forming the highly ordered helical assemblies. Of the 16 cysteine residues found in AHSV NS1 9 are conserved at the same site in BTV NS1 (Maree & Huismans, 1997). Mutational analysis of BTV NS1 revealed that both the conserved cysteines at residues 337 and 340 as well as the N- and C-termini are essential for tubule formation (Monastyrskaya *et al.*, 1994). The exact function of NS1, and the tubular structures formed by this protein, is not yet clear but studies on BTV NS1 suggest an involvement

in virus morphogenesis (Owens *et al.*, 2004). The use of the tubular structures of NS1 as an immunogen delivery system is being investigated (Ghosh *et al.*, 2002a; Ghosh *et al.*, 2002b; Murphy & Roy, 2008).

AHSV NS2 is encoded by segment 8 and is highly conserved (Van Staden & Huismans, 1991). The protein forms dense granular bodies in recombinant baculovirus infected cells (Uitenweerde *et al.*, 1995). These structures are similar to the virus inclusion bodies (VIBs) observed in the cytoplasm of AHSV infected cells. VIBs are the virus factories where viral replication and core assembly occur. NS2 is therefore believed to be involved in virus assembly by forming a matrix within the cytoplasm to which cores, viral proteins and ssRNA rapidly associate and where core assembly occurs. AHSV NS2 furthermore has ssRNA binding ability and is therefore thought to be directly involved in viral mRNA recruitment to these inclusion sites (Uitenweerde *et al.*, 1995). BTV NS2 has been found to recognise different RNA structures and to contain several RNA-binding domains. This may be the basis for the discrimination between viral RNAs and may explain how a single copy of each RNA segment is selected for incorporation into cores during virus assembly (Fillmore *et al.*, 2002; Butan *et al.*, 2004; Lymperopoulos *et al.*, 2006). NS2 is the only phosphorylated viral protein in infected cells (Devaney *et al.*, 1988). In BTV phosphorylation of NS2 is necessary for VIB formation. De-phosphorylation of the protein is thought to result in the disassembly of VIBs allowing the release of assembled cores for the attachment of the outer capsid proteins and subsequent viral release (Modrof *et al.*, 2005; Kar *et al.*, 2007).

NS3 and NS3A are encoded by the smallest RNA genome segment, S10, from alternative start codons in the same open reading frame (Van Staden & Huismans, 1991). NS3 contains 10 additional N-terminal amino acids (aa) that are absent in NS3A. Conserved regions within NS3 include: (i) the initiation codon for NS3A, (ii) a proline-rich region between aa 22 and 34, (iii) a highly conserved region (CR) between aa 46 and 90 (iv) two hydrophobic domains (HD) from aa 116-137 and 154-170 proposed to be transmembrane regions (TM) (Van Staden *et al.*, 1995) and (v) a highly variable, hydrophilic region (aa 139-158) between the HDs (Van Niekerk *et al.*, 2003; Quan *et al.*, 2008). These conserved domains are also present in NS3 from other orbiviruses, such as BTV and EEV (Van Niekerk *et al.*, 2003).

NS3 is a membrane associated protein expressed at low levels in infected cells (Van Staden *et al.*, 1995). The protein is proposed to be involved in virus release based on its presence at sites of membrane damage and virus exit in AHSV-infected cells (Stoltz *et al.*, 1996). When expressed in insect cells NS3 causes a cytotoxic effect (Van Staden *et al.*, 1995). The mechanism by which NS3 causes cell death is unknown, but may be as a result of the modification of the permeability of the cell membrane. Cytotoxicity was found to be dependant on the membrane association of

the protein, which is mediated by its two hydrophobic transmembrane domains (Van Niekerk *et al.*, 2001a). The cytotoxic nature of NS3, and its potential role in virus release, suggests a possible involvement in pathogenicity and virulence.

Unlike NS1 and NS2, NS3 is a highly variable protein with amino acid variation of up to 28% within and 37% across serotypes (Van Niekerk *et al.*, 2001b). This makes NS3 the second most variable AHSV protein after the outer capsid protein VP2. The reason for this high level of variation is unknown. Comparison of the nucleotide sequence of S10 revealed the presence of three distinct phylogenetic groups, termed clades α, β and γ (Sailleau *et al.*, 1997; Martin *et al.*, 1998; Van Niekerk *et al.*, 2001b; Quan *et al.*, 2008). Analysis of reassortant AHSV viruses indicated that the origin of the S10 gene, i.e. whether it groups into the α, β or γ clade, could contribute to the virulence phenotype and release characteristics of the virus (Martin *et al.*, 1998; O'Hara *et al.*, 1998).

Since NS3 is the focus of this investigation the functional analogues in other members of the *Reoviridae* family, namely BTV NS3 and rotavirus NSP4, will be discussed in the following sections.

1.4. BLUETONGUE VIRUS NS3

BTV NS3 is the cognate protein to AHSV NS3 in the prototype orbivirus, BTV. This orbivirus has been extensively studied and the findings have served as a model and directed research on related dsRNA viruses. A brief outline of the findings with regard to the life cycle of BTV, and the role played by the various BTV proteins, will therefore firstly be given here.

1.4.1. BTV life cycle

During the BTV life cycle cell attachment, and cell tropism, are mediated by the binding of VP2 to a cellular receptor in susceptible cells (Hassan & Roy, 1999). The virus then enters the cell through clathrin-mediated endocytosis and is incorporated into early endosomes (Forzan *et al.*, 2007). The low pH environment within these endosomes causes degradation of VP2 and triggers conformational modifications in VP5 that allow the protein to associate with and possibly permeabilise the endosomal membrane (Hassan *et al.*, 2001). This is thought to facilitate the release of the transcriptionally active core into the cytoplasm while VP5 is retained in the endosomes (Forzan *et al.*, 2007). The core particle consists of a protective layer of VP7 and VP3 proteins, the enzymes (VP1, VP4 and VP6) necessary for transcription, capping and helicase activity, and the ten dsRNA genome segments. Once in the cytoplasm the core enzymes

immediately initiate transcription of each of the genome segments into full-length positive sense ssRNA. The newly synthesised methylated and capped mRNA strands exit the core, are translated by the host cell machinery and used as templates for negative strand synthesis during the formation of the progeny virus genome (Mertens & Diprose, 2004).

Following viral protein synthesis, phosphorylated NS2 condenses with viral ssRNA to form viral inclusion bodies (VIBs). The core structural proteins localise to these VIBs where they form subcores and cores. The ssRNA is packaged within these cores and converted to dsRNA (Mertens & Diprose, 2004). During the final stages of virus assembly the outer capsid proteins, VP2 and VP5, are attached to the cores at the surface of VIBs. De-phosphorylation of NS2 in the VIBs then leads to the release of the newly formed progeny virions (Modrof *et al.*, 2005). An alternative model for the final stages of virus production was recently proposed, where VP5 associates with lipid rafts in the plasma membrane, and core particles are transported to these sites for the final assembly of the outer capsid proteins (Bhattacharya & Roy, 2008). Once the outer capsid is attached the viral protein NS3 has been proposed to mediate release by a variety of mechanisms as will be discussed in the following section.

1.4.2. Role of BTV NS3 in the viral life cycle

The smallest genome segment of BTV, as in AHSV, encodes two related proteins NS3 and NS3A from two overlapping in-phase open reading frames (Van Dijk & Huismans, 1988). BTV NS3 sequences however, in contrast to AHSV NS3, are highly conserved amongst serotypes (Van Niekerk *et al.*, 2003; Balasuriya *et al.*, 2008). Variation of BTV NS3 is thought to be limited by structural and functional constraints (Pierce *et al.*, 1998; Balasuriya *et al.*, 2008). Recombinant baculovirus expressed BTV NS3 and NS3A reacted strongly with sera from sheep following infection with homologous and heterologous BTV serotypes, suggesting that they are highly conserved group-specific antigens (French *et al.*, 1989).

BTV NS3 and NS3A are integral membrane glycoproteins (Wu *et al.*, 1992) associated with lipid membranes in infected cells (Hyatt *et al.*, 1991; Bansal *et al.*, 1998). Electron microscopic examination of BTV-infected cells showed that NS3 was associated with areas of membrane perturbation and that the presence of the protein correlated with BTV release (Hyatt *et al.*, 1991). Recombinant baculovirus expression of BTV virus-like particles (VLPs) together with NS3/NS3A resulted in the budding and release of these particles from infected cells. Release of VLPs did not occur in the absence of NS3, or when NS1 was co-expressed with the VLPs. NS3 is therefore involved in the release of BTV from infected cells (Hyatt *et al.*, 1993).

BTV may be released from cells by lysis or budding, and several studies have implicated NS3 in both release strategies. Beaton *et al.* (2002) showed that the C-terminal domain of NS3 interacts with the outermost BTV capsid protein VP2, while an amphipathic α-helix in the N-terminal domain interacts with a cellular protein p11 (currently called S100A10). The p11 protein, together with p36 (currently called annexin A2), forms a heterotetramer molecule known as the annexin II complex (or Calpactin complex). Annexins, such as annexin A2, exhibit binding to phospholipids and membranes in various tissues while S100A10 has the ability to bind cytoskeletal proteins, such as actin. The annexin II complex can therefore link membranes and/or vesicles to cytoskeletal proteins and so regulate membrane organisation (Miwa *et al.*, 2008). This complex has been implicated in cellular processes such as exocytosis and correct trafficking of proteins out of the cell. NS3 was found to interact with p11 at the same site as p36 thereby outcompeting this molecule. The addition of a peptide representing the 14 N-terminal aa of NS3 to BTV-infected C6/36 insect cells severely reduced the amount of virus released, confirming the physiological relevance of the interaction between NS3 and p11. A model for the NS3-mediated non-lytic release of BTV was therefore proposed (Fig. 1.1). In this model NS3 enables virus egress by acting as a receptor for assembled virions and recruiting them to the existing host cell export machinery (Beaton *et al.*, 2002).

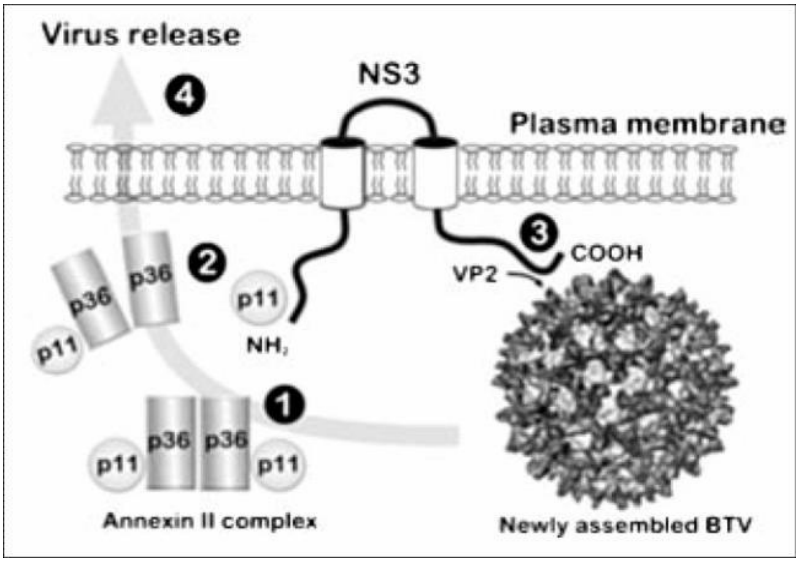

Fig.1.1 A model for the role of BTV NS3 in virus release (Beaton *et al.*, 2002). (1) p11 and p36 form a heterotetramer known as the annexin II complex involved in cellular exocytosis. (2) The N terminus of NS3 interacts with p11, either alone or it may displace one copy of p36 in the heterotetramer so forming a partial annexin II complex. (3) Newly assemble mature virions bind to NS3 via an interaction between the C terminus of NS3 and the outer capsid protein VP2. (4) The virions can now engage with the exocytic machinery via contact with the p11/annexin II complex and non-lytic virus release occurs.

An additional route for the non-lytic release of BTV was proposed when it was found that NS3 binds to and co-localises with Tsg101. This protein forms part of the ESCRT-I (endosomal sorting complex required for transport) complex in the vacuolar protein sorting (VPS) pathway. BTV NS3 interacts with Tsg101 of both mammalian and insect origins, and the interaction is mediated by a conserved PSAP late-domain motif in the conserved proline rich region of NS3. Furthermore, knockdown of Tsg101 by small interfering RNA (siRNA) in BTV-infected cells resulted in a significant reduction in the amount of virus released (Wirblich *et al.*, 2006). BTV NS3 therefore interacts with multiple cellular release factors so facilitating virus budding from infected cells (Fig.1.2).

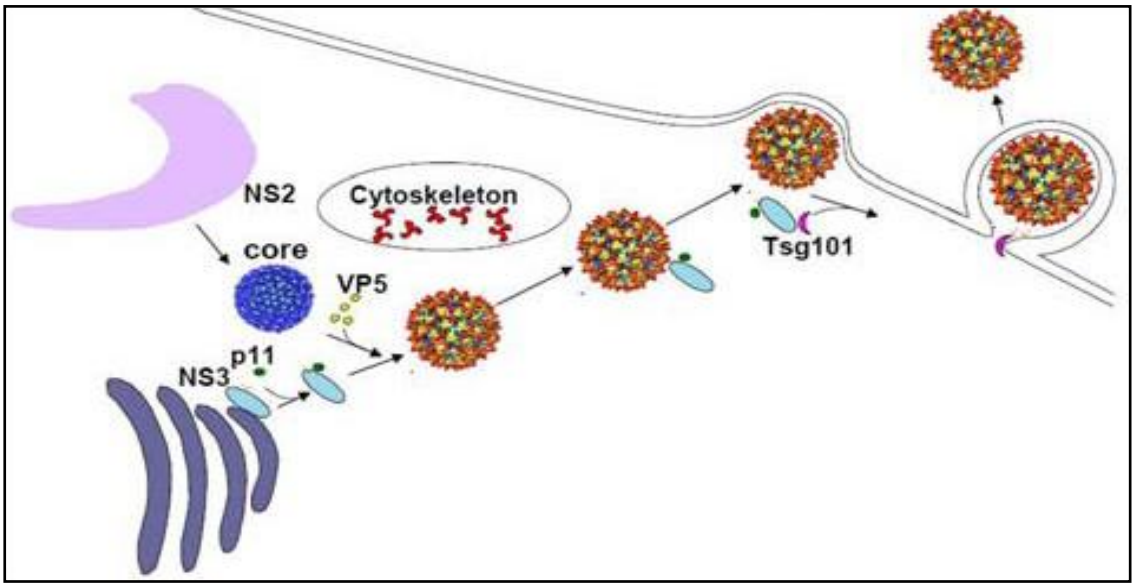

Fig.1.2 A schematic representation of how NS3 may facilitate the non-lytic release of BTV from infected cells through its interaction with the cellular release factors, p11 and Tsg101, and the BTV outer capsid protein VP2 (Roy, 2008).

Han and Harty (2004) demonstrated that NS3 forms homo-oligomers, increases membrane permeability and is targeted to the Golgi apparatus and plasma membrane of cells. The integrity of TM1, but not TM2, was found to be critical for both Golgi targeting and plasma membrane permeabilisation. They concluded that NS3 has viroporin-like properties that may contribute to the role of NS3 in lytic virus release through destabilisation of the plasma membrane. This activity may also contribute to cytopathicity in infected cells and viral pathogenesis.

It has recently been proposed that NS3 may additionally play a role in the final steps of virus assembly through its interaction with VP2 (Beaton *et al.*, 2002) and VP5, where it may keep the two outer capsid proteins in close proximity for assembly onto cores (Bhattacharya & Roy, 2008).

1.5. ROTAVIRUS NSP4

Rotavirus is a member of the *Reoviridae* family and has been the focus of much investigation because of its devastating impact on human health. The rotavirus encoded protein NSP4 is the cognate protein to NS3 of orbiviruses and may share many functional similarities to these proteins. The findings regarding this protein and the role that it plays in the viral life cycle will therefore be discussed here.

NSP4 (encoded by rotavirus genome segment 10) is a relatively small protein, the full length protein being only 175 aa. Structural domains within the protein include: (i) two high mannose N-glycosylation sites at asparagines 8 and 18, (ii) three HDs (H1, H2 and H3) (aa 1-85), (iii) a single membrane spanning or transmembrane domain (formed by H2), (iv) an α-helical coiled-coil structure that allows NSP4 to assemble into homotetramers (between aa 95-137) and (v) a relatively long cytoplasmic tail (aa 45-175) (Taylor *et al.*, 1996; Estes, 2001). The cytoplasmic tail or C-terminal region contains many of the domains responsible for the functions assigned to NSP4.

NSP4 varies by 19.4% between serotypes (Kirkwood & Palombo, 1997) which is significantly less than that observed within the AHSV NS3 protein (Van Niekerk *et al.*, 2001b). Sequence analysis of NSP4 from human and animal rotaviruses has revealed the presence of 4 distinct genetic groups or alleles, termed NSP4 genotypes A to D (Ciarlet *et al.*, 2000).

NSP4 was first identified as a glycosylated 28 kDa integral membrane protein in the ER membrane (Estes, 2001). The protein has subsequently been identified in and associated with a variety of compartments and structures within cells including the ER-Golgi intermediate compartment, autophagosomes (Berkova *et al.*, 2006), raft membranes such as the plasma membrane caveolae (Storey *et al.*, 2007) and microtubules (Xu *et al.*, 2000). NSP4 has also been found to be secreted from rotavirus-infected cells. Both a 7 kDa cleavage product of NSP4 (aa 112-175) (Zhang *et al.*, 2000) and a novel soluble form of NSP4 that has undergone additional posttranslational modifications (Bugarcic & Taylor, 2006) were identified in the media of infected cells. The protein is therefore both cell-associated (intracellular NSP4, iNSP4) and secreted from cells (extracellular NSP4, eNSP4). The fact that NSP4 has different forms, and is localised to different regions within and outside the cell, allows the protein to serve multiple functions during infection.

NSP4 has been found to play several pivotal roles during both rotavirus morphogenesis and rotavirus-induced pathogenesis (Estes, 2001). A putative role for NSP4 in modulating rotavirus

replication was also proposed when it was found that NSP4 depletion by siRNA caused a significant increase in viral transcription late in the infection cycle (Silvestri *et al.*, 2005). How NSP4 aids morphogenesis and contributes to pathogenesis will be discussed in greater detail in the following sections.

1.5.1. Role of NSP4 in rotavirus morphogenesis

During rotavirus morphogenesis immature double layered particles (DLPs) are synthesised within viroplasms in the cytoplasm. These DLPs must then bud into the ER where the final steps of virus maturation occur yielding infectious triple-layered particles (TLPs). In the ER membrane NSP4 is anchored in such a way that the C-terminus projects into the cytoplasm. This cytoplasmic tail acts as a receptor for newly synthesised DLPs and facilitates their translocation into the ER lumen (Estes, 2001). This receptor activity is mediated by the interaction between the last 17 to 20 aa of NSP4 and VP6 in the DLP (O'Brien *et al.*, 2000). When NSP4 synthesis is blocked in rotavirus infected cells almost no viral particles are assembled. The levels and distribution of several other viral proteins, including VP6, are also severely affected (Lopez *et al.*, 2005).

During budding into the ER DLPs acquire a transient lipid envelope that contains NSP4 and the outer capsid protein VP7. Once inside the ER the lipid envelope and NSP4 are lost allowing for the condensation of VP7 and the assembly of the outer capsid layer. In the mature virus the glycoprotein VP7 forms a smooth surface from which VP4 projects as spike-like structures (Estes, 2001). The stage at which VP4 is incorporated into the virion is not yet clear and may differ in different cell lines. Rotavirus assembly and release has been studied most extensively in MA104 (a rhesus monkey epithelial cell line) cells. Here most if not all of the final steps of virus assembly occur in the ER, where the incorporation of VP4 is thought to coincide with budding (Maass & Atkinson, 1990). Mature viruses then remain associated with the ER until being released by cell lysis (Estes, 2001). An alternative mode of virus assembly and release was however observed in Caco-2 cells, a well differentiated polarised cell line of human intestinal origin (Jourdan *et al.*, 1997; Sapin *et al.*, 2002).

Jourdan and co-workers (1997) found that the release of rotavirus from polarised intestinal Caco-2 cells occurred prior to any cell lysis, did not involve the Golgi apparatus or lysosomes and that the virus was associated with smooth vesicles within the cell. Sapin *et al.* (2002) later showed that VP4 associates with rafts (specialized membrane microdomains enriched in cholesterol and sphingolipids) within these cells as early as 3 hours post infection, and at a later stage other structural proteins and NSP4 were also found in these rafts. Rafts purified from these cells

contained infectious virus. In these cells, VP4 assembly with the rest of the viral particle occurs outside the ER via an association of VP7-coated DLPs with VP4-containing lipid rafts at the plasma membrane (Delmas *et al.*, 2004a; Delmas *et al.*, 2004b). Besides serving as platforms for the final stages of virus assembly these lipid rafts may also provide targeting of the mature virus to the cell membrane in a pathway that bypasses the Golgi apparatus, the classic exocytic pathway (Sapin *et al.*, 2002; Chwetzoff & Trugnan, 2006).

Several lines of evidence have shown that some portion of NSP4 resides in cellular lipid rafts; Triton X-100 resistant lipid rafts from rotavirus-infected Caco-2 cells contained NSP4 (Sapin *et al.*, 2002; Cuadras *et al.*, 2006), NSP4 (aa 114 to 135) has been shown to bind to caveolin-1, a marker of detergent resistant membrane fractions called caveolae (Parr *et al.*, 2006; Mir *et al.*, 2007), and full-length NSP4 has been detected in plasma membrane caveolae (Storey *et al.*, 2007). NSP4 within these rafts may function as a receptor to recruit DLPs and other viral proteins. VP7, NSP4 and VP4 have been shown to form complexes (Maass & Atkinson, 1990), and NSP4 binds VP4 (mediated by aa 112-148) (Au *et al.*, 1993). Furthermore, NSP4 silencing decreased the association of virus particles with rafts (Cuadras *et al.*, 2006). Rafts may also serve as a transport mechanism for NSP4 from the ER to the plasma membrane (Storey *et al.*, 2007).

NSP4 has also been shown to interact with parts of the ER molecular chaperone and folding systems. NSP4 binds to protein disulphide isomerase (PDI) (Mirazimi & Svensson, 1998) and calnexin (Mirazimi *et al.*, 1998), and also upregulates BiP (GRP78) and endoplasmin (GRP94) (Xu *et al.*, 1998). The main function of these molecular chaperones and folding enzymes is to prevent any non-specific interactions between newly synthesised proteins, to maintain these proteins in a proper state for folding and to mark incorrectly folded proteins for degradation. These proteins thus act as a quality control checkpoint in the ER. The significance of the interaction between NSP4 and this system to virus assembly is unknown but siRNA silencing of these chaperones during rotavirus infection has shown them to be necessary for quality control during rotavirus morphogenesis from MA104 cells (Maruri-Avidal *et al.*, 2008).

1.5.1. Role of NSP4 in rotavirus pathogenesis

The key pathological feature of rotavirus infection is age-dependant diarrhoea. The development of diarrhoea is a multifactorial process involving changes in the Ca^{2+} dependant processes of water and electrolyte secretion, as well as the induction of cell death in the different cell types that form the intestinal epithelium. Several properties of NSP4 have implicated this protein as a virulence factor involved in rotavirus pathogenesis. These include the ability to induce diarrhoea

in the absence of other viral proteins, increase cytosolic calcium ion concentration, induce the expression of nitric oxide synthase, destabilise membranes and disorganise the cell cytoskeleton. Each of these activities and their potential role in pathogenesis will be discussed here.

The most significant finding linking NSP4 to pathogenesis was the discovery that purified NSP4 alone induced diarrhoea when administered to young mice (Ball *et al.*, 1996). Antibodies directed against NSP4 have, furthermore, been found to block both rotaviral- and NSP4-induced diarrhoea in mice (Hou *et al.*, 2008). This enterotoxic activity is associated with a region of the protein between aa 114-135. A peptide representing this region was sufficient to illicit the same diarrhoea inducing effect as the full length protein (Ball *et al.*, 1996), and site-directed mutations between aa 131 and 140 caused a loss of function. NSP4 from virulent and avirulent rotaviruses, that had aa changes in this region, were found to differ greatly in their diarrhoea inducing activities (Zhang *et al.*, 1998). This region interacts with membranes but does not cause membrane destabilisation (Huang *et al.*, 2004). The mechanism of induction of diarrhoea by eNSP4 is believed to be a result of the activation of signal transduction pathways, such as phospholipase C-IP_3, that increases intracellular calcium levels and leads to chloride secretion. A recent study showed that NSP4 binds to integrin alpha1 and alpha2 on the surface of polarized intestinal epithelial (Caco-2) cells triggering this signalling cascade (Seo *et al.*, 2008).

Intracellular expression of NSP4, as a recombinant in insect or mammalian cells, was found to result in an increase in cytoplasmic Ca^{2+} concentration (Tian *et al.*, 1994; Berkova *et al.*, 2003). Silencing NSP4 expression in infected cells prevented the increase in cytosolic Ca^{2+} and plasma membrane permeability to Ca^{2+} normally observed during rotavirus infection and decreased virus yield by more than 90% (Zambrano *et al.*, 2008). The mechanism by which iNSP4 increases plasma membrane permeability to Ca^{2+} is currently unknown. This activity is however known to be independent of the phospholipase C-IP_3 signal transduction pathway used by eNSP4 (Tian *et al.*, 1994; Berkova *et al.*, 2003).

Expression of NSP4 in mammalian (Newton *et al.*, 1997) and *E. coli* (Browne *et al.*, 2000) cells has profound effects on cell viability and membrane stability. This membrane destabilising activity is associated with a membrane-proximal region (residues 48-91) which includes a potential cationic amphipathic helix. It has been proposed that this may be the mechanism used by iNSP4 to increase membrane permeability to Ca^{2+} (Ruiz *et al.*, 2005). Ruiz and co-workers (2005) showed that when glycosylation and membrane trafficking in rotavirus-infected cells where blocked, by tunicamycin and brefeldin A respectively, the increase in Ca^{2+} permeability was inhibited. This indicated that a glycosylated membrane targeted protein was responsible for this activity, the most likely candidate being NSP4.

Both intra- and extracellular NSP4 therefore affect Ca^{2+} homeostasis in cells. The concentration of Ca^{2+} in cells is normally tightly regulated as it controls many essential processes within the cell. Modification of Ca^{2+} homeostasis has been related to cytotoxicity and cell death, and is probably the root cause of the cytopathological effects induced by infection. Alterations to Ca^{2+} concentrations may also be part of the basis of the physiological alterations in the intestine induced by rotavirus which finally lead to diarrhoea (Zambrano *et al.*, 2008).

NSP4 may also alter aqueous secretion in intestinal cells through its ability to inhibit the Na-D-glucose symporter SGLT1 involved in water resorption (Halaihel *et al.*, 2000) and also by inducing the expression of nitric oxide (NO) synthase; an enzyme responsible for the synthesis of NO which is a possible modulator of aqueous secretion (Borghan *et al.*, 2007).

NSP4 has also been found to bind to as well as rearrange different components of the cell cytoskeleton. The protein has been identified along microtubule-like structures and found to block membrane trafficking along microtubules between the ER and the Golgi (Xu *et al.*, 2000). Expression of NSP4 has been found to increase F-actin levels and induce actin rearrangement (Berkova *et al.*, 2007). Both of the above activities may contribute to pathogenesis by interfering with cellular processes dependant on the cytoskeleton, such as endo- and exocytosis, receptor internalization, channel activity and ion gradients.

NSP4 is thus a striking example of not only how multiple functions can be mediated by a single relatively small protein, but also of how a single viral protein can significantly influence, and indeed may be the major determinant of, viral cytopathology and pathogenesis.

1.5. ALTERATION OF MEMBRANE PERMEABILITY BY ANIMAL VIRUSES

Cytolytic animal viruses induce severe adverse effects on susceptible host cells, resulting in profound morphological and biochemical changes, and eventual cell degeneration. These detrimental effects have been linked to the alteration of the host cell membrane permeability, a feature typically observed during viral infection of mammalian cells (Carrasco, 1995).

Increased permeability of the cell to ions and low-molecular-weight compounds changes the cellular ion homeostasis, disrupts the membrane potential and allows the release of essential compounds from the cell. Besides the consequences for the infected cell, membrane permeabilisation can play numerous functions in the viral life cycle. The alteration of ion concentration within the cell may promote viral protein synthesis. The translation of mRNAs from

several cytolytic animal viruses has been found to be fairly resistant to high sodium concentrations with the result that translation of viral mRNA may be promoted over cellular mRNA translation (Garry *et al.*, 1979). Changes in ion concentration may provide an ideal environment for virion assembly. The disruption of the cell membrane could facilitate virus budding and virus spread to surrounding cells. Disorganisation of cellular membranes may lead to the development of the cytopathic effect (CPE) and subsequent cell lysis (Carrasco, 1995; Gonzalez & Carrasco, 2003). Changes in cell homeostasis have also recently been implicated in modulating the cell death programme (Franco *et al.*, 2006).

Several viral gene products may be directly or indirectly responsible for this activity, including viral proteases and glycoproteins. For naked viruses, the intracellular accumulation of viral particles and the expression of large amounts of viral products have often been thought to cause non-specific membrane damage possibly leading to enhanced permeability, cell lysis and release of new progeny. However, increasing evidence has indicated that in a large number of animal viruses a single cytotoxic viral protein or viroporin is specifically responsible for the modification of membrane integrity at late stages of infection (Gonzalez & Carrasco, 2003). Viroporins are virus encoded proteins that when expressed individually cause an increase in membrane permeability to ions and other small molecules (Carrasco, 1995). Several endomembrane systems within the cell may be affected, including the plasma membrane, the ER and the Golgi complex. Examples of viroporins are given in Table 1.1.

Table 1.1 List of viroporins (modified from Gonzalez & Carrasco, 2003)

Virus family	**Viroporins**
Togaviridae	SFV (Semliki forest virus) 6K, Sindbis virus 6K, Ross River virus 6K
Picornaviridae	Poliovirus 2B, Coxsackievirus 2B, Poliovirus 3A
Retroviridae	HIV-1 (human immunodeficiency virus type 1) Vpu
Paramyxoviridae	HRSV (human respiratory syncytial virus) SH
Orthomyxoviridae	Influenza A virus M2
Reoviridae	ARV (avian reovirus) p10
Flaviviridae	HCV (Hepatitis C virus) p7
Phycodnaviridae	PBCV-1 (*Paramecium bursaria* chlorella virus) Kcv
Rhabdoviridae	BEFV (bovine ephemeral fever virus) alpha 10p
Coronaviridae	MHV (murine hepatitis virus) E, SARS-CoV (severe acute respiratory syndrome coronavirus) E

Viroporins are typically small proteins (60-120 aa) that interact directly with membranes. A variety of structural features identified in viroporins may then contribute to the destabilisation of the membrane. The best characterised viroporins are integral membrane proteins that contain a hydrophobic domain that forms an amphipathic α-helix. Upon insertion into the membrane, and oligomerisation of the protein, the hydrophilic residues in this amphipathic helix form a hydrophilic pore, while the hydrophobic residues interact with phospholipids in the membrane. Other viroporins contain an additional hydrophobic domain that interacts with and potentially disturbs the lipid bilayer. The presence of basic amino acids within or surrounding the hydrophobic domain in some viroporins may furthermore have a detergent like effect on membranes (Gonzalez & Carrasco, 2003).

Selected examples of viroporins, and their role in the viral life cycle, will be discussed in the following section.

6K proteins of alphaviruses

Sindbis virus and Semliki forest virus are enveloped, positive sense RNA cytolytic viruses of animals in the *Alphavirus* genus. Late in Sindbis virus infection an increase in intracellular Na^+ ion concentration occurs as a result of changes in cell permeability. This correlates with a substantial decrease in host protein synthesis, while virus protein synthesis continues and appears to favour these conditions (Ulug *et al.*, 1996). These intracellular conditions, therefore, lead to the preferential expression of the virus proteins over the host cell proteins. Changes in the permeability of the membrane of infected cells have been associated with an accessory protein named 6K protein.

6K proteins are small hydrophobic α-helical proteins that associate with membranes. In eukaryotic cells the expression of 6K increases membrane permeability to the translation inhibitor Hygromycin B (Sanz *et al.*, 2003; Madan *et al.*, 2005b; Madan *et al.*, 2008). Inducible expression in *E. coli* leads to leakage of the bacterial cell membrane and cell death (Sanz *et al.*, 1994). 6K proteins, produced synthetically or in *E. coli*, are incorporated into planar lipid bilayers forming cation selective ion channels, increasing membrane conductance (Melton *et al.*, 2002).

Reverse genetics studies on Semliki forest virus, where the entire gene encoding the 6K protein was deleted, indicated that virus replication was not abrogated but that the final assembly and budding of progeny virions were defective. In the absence of 6K virus binding, internalisation, uncoating, replication and the formation of nucleocapsids occurred, but the newly formed nucleocapsids accumulated at the plasma membrane (Loewy *et al.*, 1995; Sanz *et al.*, 2003). In

HIV-1 mutants expressing truncated variants of the HIV-1 viroporin, Vpu, a similar effect was noted. Here the virus was still capable of replication but the final assembly and exit of virus particles was affected with a large proportion of particles remaining cell associated (Gonzalez & Carrasco, 2001). Interestingly, the synthesis of HIV-1 Vpu in cells infected with Sindbis virus lacking the 6K gene was capable of compensating for, in part, the defects in final assembly and release caused by the absence of 6K (Gonzalez & Carrasco, 2001).

2B proteins of enteroviruses

Enteroviruses (such as poliovirus, coxsackievirus, echovirus) are members of the *Picornaviridae* family of nonenveloped, cytolytic viruses. Several functional and morphological modifications occur in host cell membranes in enterovirus infected cells. The permeability of both intracellular membranes and the plasma membrane is affected, and the enterovirus viroporin 2B protein plays a major role in these virus-induced membrane modifications (Aldabe *et al.*, 1996; De Jong *et al.*, 2004). Recombinant expression of 2B in mammalian cells induces the permeabilisation of the plasma membrane, the ER and the Golgi complex (Aldabe *et al.*, 1996; Van Kuppeveld *et al.*, 2005). 2B localises to the ER, Golgi complex and to a lesser extent to the plasma membrane (De Jong *et al.*, 2004). The 2B protein sequence contains two hydrophobic domains, predicted to form transmembrane regions that insert into the negatively charged membranes of the target organelles forming an integral hairpin loop (De Jong *et al.*, 2004).

The 2B protein of enteroviruses additionally has an anti-apoptotic function that is related to its membrane permeabilising effect. The 2B protein forms pores in the ER and Golgi membranes allowing the passage of Ca^{2+} out of these organelles thereby reducing their Ca^{2+} content. This potentially serves two different purposes. Firstly, it provides the intracellular conditions necessary for the replication of the viral RNA genome, and secondly delays the apoptotic host-cell response. ER–mitochondrial Ca^{2+} signalling occurs during the initiation of apoptosis, the reduction of calcium in the ER and Golgi by 2B therefore perturbs this signalling pathway. This activity delays the host-cell apoptotic response allowing time for the virus to replicate. The apoptotic program is not, however, blocked and at a later stage the killing of the host cell facilitates the release of the newly formed progeny virions (Van Kuppeveld *et al.*, 2005). Madan *et al.* (2008) however report that several viroporins from RNA viruses, including the 2B protein of poliovirus, are capable of inducing apoptosis when expressed individually in BHK cells. They propose that during the initial stages of virus infection, when the levels of 2B are low, apoptosis is inhibited allowing for virus replication. At later stages when expression levels of 2B are higher apoptosis is induced. This may then provide a means for the efficient spread of virions that evades the host immune inflammatory response.

E proteins of coronaviruses

The E protein from the coronaviruses, murine hepatitis virus and severe acute respiratory syndrome coronavirus (SARS-CoV), has recently been shown to have viroporin activity. The expression of the E protein permeabilises both *E. coli* and mammalian cells (Madan *et al.*, 2005a; Liao *et al.*, 2006). The protein also displays structural features characteristic of viroporins, with a highly hydrophobic domain that forms at least one amphipathic α-helix (Liao *et al.*, 2006).

Studies in which the entire ORF encoding the E protein was removed, showed that the E protein was not required for virus replication as viable and infectious progeny were produced. The titres of mutant virus were, however, greatly reduced with respect to the wild-type virus, suggesting that virion assembly or morphogenesis was less efficient and that the E protein increases assembly rate (Kuo & Masters, 2003; DeDiego *et al.*, 2007). Mutant Influenza A viruses, in which the M2 transmembrane domain responsible for ion channel activity was deleted, were also able to undergo multiple cycles of replication but grew substantially slower. This indicates the importance of M2 ion channel activity in the rate of efficient viral replication (Watanabe *et al.*, 2001). Therefore, in some cases, the expression of viroporins has been found not to be essential for progeny virus formation, their expression, however, significantly increases virus production suggesting a putative role in modulating virus production.

Recent studies have proposed that AHSV NS3 (Van Niekerk *et al.*, 2001a), BTV NS3 (Han & Harty, 2004) and rotavirus NSP4 (Ruiz *et al.*, 2005) may have viroporin-like activity based on their cytotoxic and/or membrane permeabilising effect when expressed individually. Further characterisation of their role during the viral life cycle has, however, been hindered due to the lack of a reverse genetics system for these segmented dsRNA viruses. Although following the onset of this study a reverse genetics system for BTV has been developed (Boyce *et al.*, 2008). In this study genomic segment reassortment was used as an alternative tool for studying protein function. This evolutionary mechanism, and its application in protein function studies, will therefore be discussed in the following section.

1.6. GENOME SEGMENT REASSORTMENT

RNA viruses are characterised by small and compact genomes, short generation times, large population numbers and the highest mutation rates amongst living species. The high mutation rate is due to the low, or absent, proof reading activity of their RNA-dependant RNA polymerases, which have an error rate of 10^{-3} to 10^{-5} misincorporations per nucleotide copied (Domingo & Holland, 1997). Genomic variation in RNA viruses is additionally generated through homologous

and nonhomologous recombination and, in those viruses with a segmented genome, reassortment or genetic drift. Reassortment is the exchange of genome segments between different virus strains co-infecting the same cell, and results in the formation of new strains or variants with segments from both viruses (reassortants). RNA viruses therefore generally evolve as a mixed population of related but non-identical genomes, with one or several master nucleotide genome sequence(s) or quasispecies dominating the population (Domingo *et al.*, 1996). This potentially provides the virus with a high adaptive potential in new environments where the selection of viral sub-populations with the highest fitness, even if they are in the minority, allows for rapid evolution (Briones *et al.*, 2006). The alternative replication in vertebrate and non-vertebrate hosts that occurs in arthropod transmitted viruses, however, imposes constraints on these viruses and they generally evolve slower, as has been demonstrated for sindbis virus (Greene *et al.*, 2005).

Genome segment reassortment has been shown to occur in nature for many segmented animal RNA viruses, including AHSV (Von Teichman & Smit, 2008), BTV (Kahlon *et al.*, 1983; Pierce *et al.*, 1998) and rotavirus (Iturriza-Gómara *et al.*, 2001). The ability of the AHSV and BTV viruses to reassort raises concerns over the current use of attenuated live vaccines for these viruses. This is due to the potential risk of reassortment with field strains and possible reversion to virulence. Field strains containing segments from vaccine strains have recently been detected for both viruses (Batten *et al.*, 2008; Von Teichman & Smit, 2008).

Reassortment of genome segments of BTV and AHSV has also been shown to occur *in vitro* (Ramig *et al.*, 1989; O'Hara *et al.*, 1998). Ramig and co-workers (1989) examined the constraints and kinetics of BTV reassortment in Vero cells. Reassortment was found to be an early event in the replication cycle, and non-random segregation of specific genome segments occurred. In the absence of selection pressures, the majority of the genome segments randomly segregate, segments 8 and 10, however, were found to segregate non-randomly with bias towards one parent. The basis for this non-random segregation is not known (Ramig *et al.*, 1989). Preferential selection of the genome segment encoding NSP1 from one of the parental viruses during mixed infection with rotaviruses has also been demonstrated (Mahbub Alam *et al.*, 2006). No studies have directly examined the constraints and kinetics of AHSV reassortment, or whether viral protein interactions or protein-protein function influence this.

The *in vitro* generation of reassortants, through mixed infections and/or reverse genetics, has proven to be a powerful tool in elucidating viral protein functions in many segmented RNA viruses such as reovirus (Moody & Joklik, 1989; Roner & Mutsoli, 2007), rotavirus (Tauscher & Desselberger, 1997), BTV (Cowley & Gorman, 1987) and influenza virus (Parks *et al.*, 2007;

Pappas *et al.*, 2008). In this type of analysis phenotypic traits in which the two parental strains differ are selected and, using either random genome segment reassortants or reassortants generated by reverse genetics, these phenotypes are then associated with the presence of specific genome segments. For example, co-segregation of the hemagglutination functions of BTV with the gene encoding the outer capsid protein VP2 in reassortants between two BTV serotypes that differed in their hemagglutination patterns, demonstrated that VP2 was the virus hemagglutinin (Cowley & Gorman, 1987). *In vitro* reassortment is also widely used for creating viruses with specific phenotypes for vaccine purposes (Dennehy, 2008) and in analysing the potential dangers of reassortment between attenuated vaccine strains and field strains (Parks *et al.*, 2007).

In a previous study AHSV reassortants were used to identify genome segments controlling virulence in a mouse model system. Two virus strains with avirulent and virulent phenotypes in adult Balb C mice were selected as parental strains for the generation of reassortants. Reassortants were then analysed for virulence in Balb C mice. Reassortant viruses clustered into three phenotypic groups; avirulent, virulent and those with a novel intermediate virulence. Genome segment 2, encoding the outer capsid protein VP2, from the virulent parent was present in all reassortant viruses displaying the virulent phenotype. Similarily all the avirulent reassortants had genome segment 2 from the avirulent parent. VP2, and its role in cell entry, may therefore have an important influence in determining the virulence characteristics of AHSV in the mouse model. Interestingly, all of the virulent reassortant strains also contained the genome segments encoding VP5 and NS3 from the virulent parent. These segments, however, could not be the primary determinants of the virulent phenotype as they also appeared in the other groups of viruses. They may however be necessary for the expression of the virulent phenotype. All the viruses with a novel intermediate virulence phenotype had VP2, VP5 and NS1 from the avirulent parent but NS3 from the virulent parent, indicating that although NS3 may not be the primary determinant of virulence in mice, the presence of NS3 from the virulent parent significantly increases virulence (O'Hara *et al.*, 1998).

1.7. AIMS

The virulence and pathogenesis of AHSV is likely to involve complex interactions between multiple viral and host determinants. Viral factors include those that control or influence key events during the viral life cycle, such as cell entry, rate of viral replication, virus trafficking and release. In addition to this, virus proteins that influence the cytopathic effects induced during viral infection, that alter cellular homeostasis, and that manipulate the host cell response to infection may also play a role in pathogenesis. Characterisation of the AHSV proteins that contribute to

these aspects is therefore of vital importance to understanding the molecular and cellular basis of AHS disease and its progression. In this study we focussed on AHSV NS3 due to the cytotoxic nature of the protein and its potential role in virus release. A further unique and intriguing feature of AHSV NS3 is the high variability of this protein within and across serotypes of AHSV. This is in contrast to BTV NS3, the other non-structural proteins of AHSV, and indeed most of the non-structural proteins of dsRNA viruses; which are often the most highly conserved of the viral proteins.

The central objective of this investigation was to further characterise the role that the AHSV NS3 protein plays in the viral life cycle and virus-cell interactions, such as cytopathology and cytotoxicity, that potentially contribute to the events leading to pathogenesis. The following specific aims were therefore addressed in this study:

1. To determine the contribution of NS3 to virus phenotypic properties such as virus yield, virus release, virus-induced cytopathicity and membrane permeabilisation during AHSV infection of mammalian cells.

2. To compare the membrane permeabilising and cytolytic effect of NS3 from AHSV, BTV and EEV.

3. To determine which regions within NS3 are critical to its membrane permeabilising and cytolytic effects.

4. To determine if sequence variation within NS3 influences its membrane permeabilising effect, cytotoxicity, membrane association and subcellular localisation.

CHAPTER 2: GENOME SEGMENT REASSORTMENT IDENTIFIES NS3 AS A KEY PROTEIN IN AHSV RELEASE AND MEMBRANE PERMEABILISATION

2.1. INTRODUCTION

The prominent pathological features of AHS are haemorrhages, oedema and effusion (Mellor & Hamblin, 2004). These features have been associated with changes in the morphology and permeability of pulmonary and vascular endothelial cells, the main target cells during AHSV infection (Laegreid *et al.*, 1992a). Infection of cultured endothelial cells with virulence variants of AHSV resulted in distinctly different cytopathologies (Laegreid *et al.*, 1992b). When grown in tissue culture AHSV causes severe cytopathic effects (CPE) in mammalian cells (Coetzer & Guthrie, 2004).

AHSV NS3, encoded by segment 10 (S10), is the smallest of the viral proteins and is expressed to low levels in infected cells (Van Staden *et al.*, 1995). Immunolocalisation studies of AHSV-infected Vero cells showed that NS3 was localised to the plasma membrane specifically at the perturbed areas at the sites of virus exit. NS3 was therefore proposed to be involved in virus release (Stoltz *et al.*, 1996). When expressed individually in insect or mammalian cells, both the AHSV and BTV NS3 proteins cause a cytotoxic effect (Van Staden *et al.*, 1995; Van Niekerk *et al.*, 2001a; Han & Harty, 2004). Cells expressing AHSV NS3 display degraded or absent cell membranes, cytotoxicity is therefore possibly as a result of membrane damage. Cytotoxicity was shown to be dependant on the membrane association of the protein, mediated by two hydrophobic domains (Van Niekerk *et al.*, 2001a). NS3 has been proposed to function as a viroporin that induces changes in membrane permeability, facilitates virus release, and possibly contributes to the cytopathic effect thereby potentially contributing to pathogenesis (Van Niekerk *et al.*, 2001a; Han & Harty, 2004). These findings have however never been investigated in the context of AHSV infection of cells. The first objective of this part of the study was therefore to investigate the functional significance of the NS3 protein in AHSV infection of mammalian cells, and, secondly, to determine whether the high levels of sequence variation in NS3 impacted on this.

In stark contrast to BTV NS3, that is highly conserved amongst different serotypes (Van Niekerk *et al.*, 2003; Balasuriya *et al.*, 2008) AHSV NS3 shows much more sequence diversity with up to 37% amino acid variation across all serotypes (Van Niekerk *et al.*, 2001b). Comparison of the nucleotide sequence of S10, the segment encoding NS3, shows that this variation clusters into three distinct phylogenetic groups, termed clades α, β and γ (Sailleau *et al.*, 1997; Martin *et al.*, 1998; Van Niekerk *et al.*, 2001b; Quan *et al.*, 2008).

To assess the role played by NS3 during AHSV infection a reassortant based approach was used. Three parental AHSV isolates, AHSV-2, AHSV-3 and AHSV-4, were selected based on the segregation of their NS3 proteins into the three phylogenetic clades (Van Niekerk *et al.*, 2001b) and preliminary observations by van Niekerk (2001c) that they differed in their cytopathology in

Vero cells. The NS3 proteins encoded by AHSV-2, AHSV-3 and AHSV-4 respectively represent the γ, β and α clades. From these parental strains, reassortant progeny viruses were generated by co-infections of cells and progeny plaque purifications. Reassortants in which genome segment 10 encoding NS3 was exchanged, with or without the exchange of additional segments, were identified on the basis of the migration of the dsRNA genome segments in PAGE gels and from partial sequencing of the genome segments. Reassortants and parental strains were then compared in Vero cells in terms of virus yield, virus release and viral-induced CPE as well as their effect on cell viability and cell membrane permeability to evaluate the contribution of the NS3 protein to viral phenotype.

2.2. MATERIALS AND METHODS

2.2.1. Cells and viruses

BHK-21 (ATCC CCL-10) and Vero (ATCC CCL-81) cells were obtained from ATCC (Manassa, USA). CER cells, a BHK derivative, were obtained from the Virology Division at the Onderstepoort Veterinary Institute (OVI, Onderstepoort, South Africa). BHK, Vero and CER cells were maintained in monolayers in minimal essential medium (MEM) supplemented with non-essential amino acids (Sigma), 5% foetal calf serum (FCS, Sigma) and antibiotics (60 mg/ml penicillin, 60 mg/ml streptomycin and 150 µg/ml fungizone, Highveld Biological). Cells were maintained at 37°C in 5% CO_2.

The parental virus strains used in this study were obtained from the OIE Reference Laboratory at the OVI. AHSV serotype 2 82/61 (AHSV-2) and AHSV serotype 4 HS39/97 (AHSV-4) were isolated from spleen or lung samples of dead horses; AHSV serotype 3 M322/97 (AHSV-3) from the spleen of a dead dog. These strains each encode a NS3 protein from one of the three NS3 phylogenetic clades, i.e. AHSV-2 (γ NS3), AHSV-3 (β NS3) and AHSV-4 (α NS3) (Van Niekerk *et al.*, 2001b). Single virus populations were obtained following three rounds of plaque purification in BHK cells.

2.2.2. Isolation of AHSV reassortants

BHK cells seeded on 6 well plates and grown to 80% confluency were co-infected with two parental strains at equal multiplicities of infection (MOI) of 1 or 4 plaque-forming units (pfu)/cell. The inoculum was replaced after 3 h with supplemented MEM. Supernatants were harvested at 2 to 3 days post infection (p.i.) and individual progeny viruses obtained by plaque purification. For this BHK cells seeded on 6 well plates were incubated for 1 h with diluted virus-containing supernatant in an equal volume supplemented MEM. The inoculum was removed, and cells overlaid with 2 ml of 0.7% agarose in MEM containing 5% FCS and antibiotics. Plaques were randomly selected after 3 to 4 days incubation at 37°C, resuspended in 1 ml complete medium, and amplified twice by passage in BHK cells as routinely done for the AHSV parental strains.

2.2.3. Genome segment assignment

2.2.3.1. Isolation and polyacrylamide gel electrophoresis (PAGE) of dsRNA

Viral dsRNA was isolated from infected BHK cells using TRIZOL reagent (Invitrogen) according to the manufacturer's recommendations. RNA samples were stored at 4°C in diethylpyrocarbonate (DEPC) treated water. Samples were analysed by 6, 8, 10, 12 and 14% polyacrylamide gel electrophoresis (PAGE) to identify the origins of the genome segments. Briefly, samples were concentrated in the spacer gel containing 3% acrylamide, 0.08% N, N' methylene bis-acrylamide, 64 mM Tris pH 6.7, 0.15% ammoniumperoxydisulphate, 0.15% TEMED. The RNA was then separated in the resolving gel containing 6, 8, 10, 12 or 14% acrylamide and 0.16, 0.21, 0.27, 0.32, or 0.37% N, N' methylene bis-acrylamide, 375 mM Tris pH 8.9, 0.0625 N HCl, 0.15% ammoniumperoxydisulphate, 0.05% TEMED). Electrophoresis was carried out in Tris-glycine buffer (25 mM Tris, 250 mM glycine) at 80-90V for 20 h. The gels were stained in Tris-glycine buffer containing SYBR gold nucleic acid gel stain (Molecular Probes) and viewed under a UV transilluminator.

2.2.3.2. Sequencing of genome segments

The total dsRNA was converted to cDNA using a single-primer amplification sequence-independent dsRNA method (Potgieter *et al.*, 2002) by Dr A. C. Potgieter, OVI. Full or partial individual gene segments were then amplified by PCR using gene specific primers for segments 2, 3, 5, 6, 7, 8, 9 and 10. All PCR reactions were carried out in a final volume of 50 µl containing 1.25 U Takara ExTaq, 5 µl 10 x Takara reaction buffer (including $MgCl_2$), 2.5 mM of each dNTP

and 100 pmol of each primer. Primer sequences and PCR conditions used are listed in Table 2.1. PCR amplicons were purified using a commercial purification kit (Roche) and sequenced using an ABI PRISM Big Dye Terminator Cycle Sequencing Ready Reaction kit with the primers in Table 2.1 on an ABI PRISM 3130xl Genetic Analyzer (Perkin Elmer). Sequences were aligned using AlignX, Vector NTI (Invitrogen).

Table 2.1 Primers used to PCR amplify and sequence individual gene segments of the AHSV strains and reassortants used in this study

Primer Name (Storage Code)	**5' to 3' sequence (Orientation)**	**Amplification product and PCR conditions**
HSV3VP2FOR (P3H1)	GTTTAATTCACCATGGCTTCGGAATTCG (Forward)	Full length VP2 gene on segment 2 of AHSV-3 94°C 4 minutes (min) 35 x (94°C 30 sec, 56°C 30 sec, 72°C 3 min) 72°C 7 min
HSV3VP2REV (P3I1)	GTAAGTTGATTCACATGGAGCGGGAG (Reverse)	
HS4VP2FOW (P3C8)	GTTAAATTCACTATGGCGTCCGAGTTG (Forward)	Full length VP2 gene on segment 2 of AHSV-4 94°C 4 min 35 x (94°C 30 sec, 57°C 30 sec, 72°C 3 min) 72°C 7 min
HS4VP2REV (P3C9)	GTATGTGTATTCACATGGAGCAACAG (Reverse)	
SI5 (P4E1)	GGAGATCTATGCAAGGGAATGAAAGAATAC (Forward)	Full length VP3 gene on segment 3 94°C 4 min 35 x (94°C 30 sec, 59°C 30 sec, 72°C 3 min) 72°C 7 min
SI3 (P4A1)	GGAGATCTGGCTGCTAAATCGTTGGTCG (Reverse)	
VP5IF3/9 (P6C1)	AGGAAGATCGTGTGATTG (Forward)	Bases 380 to 1160 of VP5 gene on segment 6 of AHSV-3 94°C 2 min 35 x (94°C 30 sec, 52°C 30 sec, 72°C 90 sec) 72°C 5 min
VP5IR3/9 (P6B1)	TGGCGTATGCTCTGAATG (Reverse)	
HS4VP5BamF (P6A1)	GTGGGATCCATGGGAAAGTTCACATC (Forward)	Full length VP5 gene on segment 6 of AHSV-4 94°C 2 min 35 x (94°C 30 sec, 53°C 30 sec, 72°C 90 sec) 72°C 5 min
HS5VP5EcoRIR (P6F1)	CGGAATTCAGCTATTTTCACACCATATAC (Reverse)	
AHSV4NS1BamFP (P9A2)	GCGGATCCGTTAAAGAACCTAGGCGG (Forward)	Full length NS1 gene on segment 5 94°C 2 min 35 x (94°C 30 sec, 59°C 30 sec, 72°C 90 sec) 72°C 5 min
AHSV4NS1EcoRP (P9A3)	CGGAATTCGTAAGTTTGTGAAACCAGGGGG (Reverse)	
VP7A (P8A3)	5' end of segment 7 AHSV9 (Forward)	Full length VP7 gene on segment 7 94°C 2 min 35 x (94°C 30 sec, 47°C 30 sec, 72°C 90 sec) 72°C 5 min
VP7B (P8B3)	3' end of segment 7 AHSV9 (Reverse)	
G8.1 (NS2F) (P10A1)	GTTTAAAAATCCGTTCGTCATC (Forward)	Full length NS2 gene on segment 8 94°C 2 min 35 x (94°C 30 sec, 54°C 30 sec, 72°C 90 sec) 72°C 5 min
G8.2 (NS2R) (P10B1)	GTATGTTGAAATCCGCGGTTA (Reverse)	

Primer Name (Storage Code)	5' to 3' sequence (Orientation)	Amplification product and PCR conditions
VP6.5 (P7A1)	GTAAGTTTTAAGTTGCCC (Forward)	Full length VP6 gene on segment 9 94°C 2 min 35 x (94°C 30 sec, 46°C 30 sec, 72°C 90 sec) 72°C 5 min
VP6.4 (P7B1)	GTTAAATAAGTTGTCTCATG (Reverse)	
NS3pBam (P11E3)	CGGGATCCGTTTAAATTATCCCTTG (Forward)	Full length NS3 gene on segment 10 94°C 2 min 35 x (94°C 30 sec, 59°C 30 sec, 72°C 60 sec) 72°C 5 min
NS3pEco (P11E4)	CGGAATTCGTAAGTCGTTATCCCGG (Reverse)	

2.2.4. Virus titration

The phenotypes of the parental and reassortant viruses, such as virus yield and release, were then assayed in Vero cells as previous characterisation of AHSV expression was carried out in Vero cells (Van Staden *et al.*, 1995; Stoltz *et al.*, 1996). Vero cells seeded on 6 well plates were infected with virus strains at a MOI of 10 pfu/cell for 1 h at 37°C. Unbound virus was removed by washing twice with cold serum free medium. Prewarmed supplemented medium was then added and the cells incubated at 37°C. At 24 or 48 h p.i. the cells were resuspended in the medium and collected by centrifugation at 380 g for 10 min. The resulting supernatant was diluted directly for plaque assays to quantify released virus. The cell pellets were resuspended in 2 mM Tris, incubated for 10 min at room temperature and lysed by passage through a 22G needle. Serial dilutions of lysates then allowed for the determination of the amount of cell-associated virus. Virus titres were determined by plaque assay, as described above, on CER cells. Plaques were visualised by staining with 1 ml/well 0.1% w/v neutral red (Fluka) for 2 h at 37°C. Total virus yield was calculated as the sum of released and cell-associated virus, and virus release expressed as the percentage released virus versus total virus.

2.2.5. Cytopathic effect (CPE) and cell viability

Vero cells were seeded on sterile glass coverslips in 6 well plates and infected at a MOI of 5 pfu/cell with virus strains as described above. Cells were examined for viral induced CPE at 12 hourly intervals over a 48 h period under an inverted phase-contrast light microscope. CPE was comparatively scored from slight (+) to severe (++++).

Cell viability was monitored using the CellTiter-Blue™ cell viability assay according to the manufacturer's instructions (Promega). This assay is based on the reduction of resazurin to the highly fluorescent resorufin by metabolically active cells. The metabolic capacity in non-viable cells is rapidly lost, they do not therefore reduce the indicator dye and no fluorescent signal is generated. Briefly, Vero cells seeded on 48 well plates were infected with virus strains at a MOI of 10 pfu/cell as described above. A volume of 50 µl CellTiter-Blue™ reagent was added per well at 6 hourly intervals from 0 to 48 h p.i. and cells incubated at 37°C for a further 3 h. Fluorescence ($530\text{-}570_{Ex}/580\text{-}620_{Em}$) was recorded using a Thermo Labsystems Fluoroskan Ascent FL plate reader. Background fluorescence was corrected for by including wells with serum supplemented MEM in the absence of cells. Fluorescence readings for these wells were subtracted from experimental wells. The percentage viable cells was calculated by expressing the fluorescence in wells containing the AHSV infected Vero cells as a percentage of the fluorescence in wells containing uninfected (mock) cells.

2.2.6. Hygromycin B (Hyg B) membrane permeability assay

Membrane permeabilisation assays were modified from the method described by Chang *et al.* (1999). Vero cells were infected on 48 well plates as described above. At 6, 12 and 18 h p.i. the

medium was removed and the cells washed twice with MEM without methionine. Cells were incubated for 30 min with MEM without methionine with or without Hygromycin B (Hyg B, 500 μg/ml, Roche Diagnostics). Proteins were labelled for 30 min in MEM without methionine with 2.5 μCi [^{35}S] L-methionine (Perkin Elmer) per well. Cells were washed twice with ice-cold PBS and harvested in 50 μl/well lysis buffer (150 mM NaCl, 50 mM Tris-HCl, 1 mM EDTA, 1% Nonidet P40 and protease inhibitors 1 mg/ml pefabloc SC, 0.7 μg/ml pepstatin, 1 mM phenylmethylsulphonyl fluoride (PMSF)). TCA solution (5% trichloroacetic acid in 20 mM sodium pyrophosphate) was added to precipitate proteins and the sample spotted onto fibreglass discs (GF/C, Whatman). Discs were washed with 70% ethanol and left to dry at room temperature. Discs were placed in scintillation fluid (Beckman) and counted in a Tri-Carb 2800TR Liquid Scintillation Analyzer (Perkin Elmer). The percentage permeabilised cells was calculated as counts per minute (CPM) of sample containing Hyg B divided by CPM of sample in absence of Hyg B x 100. The CPM of samples labelled in the absence of Hyg B was used a measure of total protein synthesis.

2.2.7. Statistical analysis

Mean and standard deviations (SD) were calculated, and differences in phenotype between Vero cells infected with AHSV strains and reassortants tested for significance by Student's *t* test. Pearson's product-moment correlation tests were used to calculate correlation coefficients.

2.3. RESULTS

2.3.1. Production and characterisation of AHSV reassortants

In order to generate reassortant viruses, cells were simultaneous infected with a combination of either parental strains AHSV-2 and AHSV-3, or AHSV-2 and AHSV-4, or AHSV-3 and AHSV-4 at an equal MOI. Progeny virus clones were plaque purified and amplified. In this study the primary aim was to determine the effect of NS3, encoded by the S10 gene, on the phenotype of AHSV so the selection of reassortants focussed on the exchange of the smallest genome segment 10 in relation to the serotype-determining segment 2 encoding VP2. Five putative reassortants were therefore initially identified based on the differential PAGE migration patterns of segments 2 and 10. Representative 14 and 6% polyacrylamide gels are shown in Fig. 2.1. Genome segment numbers are given based on the order of migration of the segments during agarose gel electrophoresis, the principal difference being that during PAGE segments 5 and 6 are often found to migrate in the reverse order (O'Hara *et al.*, 1998).

The parental origin of all of the genome segments of the reassortants were then identified on the basis of their PAGE profiles, and/or from partial sequencing of the genome segments following cDNA synthesis and PCR amplification of the complete genomes (see 2.2.3.2).

Table 2.2 lists the dsRNA genome segments that could be distinguished by PAGE. Segments 1 and 4 were not sequenced as their parental origins could be assigned based on their PAGE profiles, and these genes are highly conserved across all AHSV serotypes. To illustrate the differences in the migration of segment 1 of the viruses an enlargement of the upper part of the 14% gel from Fig. 2.1A is shown in Fig. 2.2. The assignment of segment 4 of reassortants between AHSV-2 and AHSV-3 was based on their differential migration during 6% PAGE, to show this an enlargement of Fig. 2.1B is given in Fig. 2.3A. PAGE analysis of the total genomic cDNA profiles of the viruses revealed that additional differences in the migration of the parental virus cDNA segments, that were not evident in the dsRNA profiles, could be distinguished. The parental origin of segment 4 of the reassortants between AHSV-2 and AHSV-4 could be assigned following 8% PAGE of the total genomic cDNA (Fig. 2.3B).

Table 2.2 The dsRNA genome segments that showed distinguishable mobility between the indicated parental strains in different percentages polyacrylamide gels

Parental strains	6% PAGE	8% PAGE	10% PAGE	12% PAGE	14% PAGE
AHSV-2 and -3	2, 4, 6, 10	2, 4, 6, 10	2, 4, 6, 10	2, 6, 10	1, 2, 6, 10
AHSV-2 and -4	2, 6, 9, 10	2, 6, 10	2, 6, 10	2, 6, 7, 10	1, 2, 6, 7,10

A

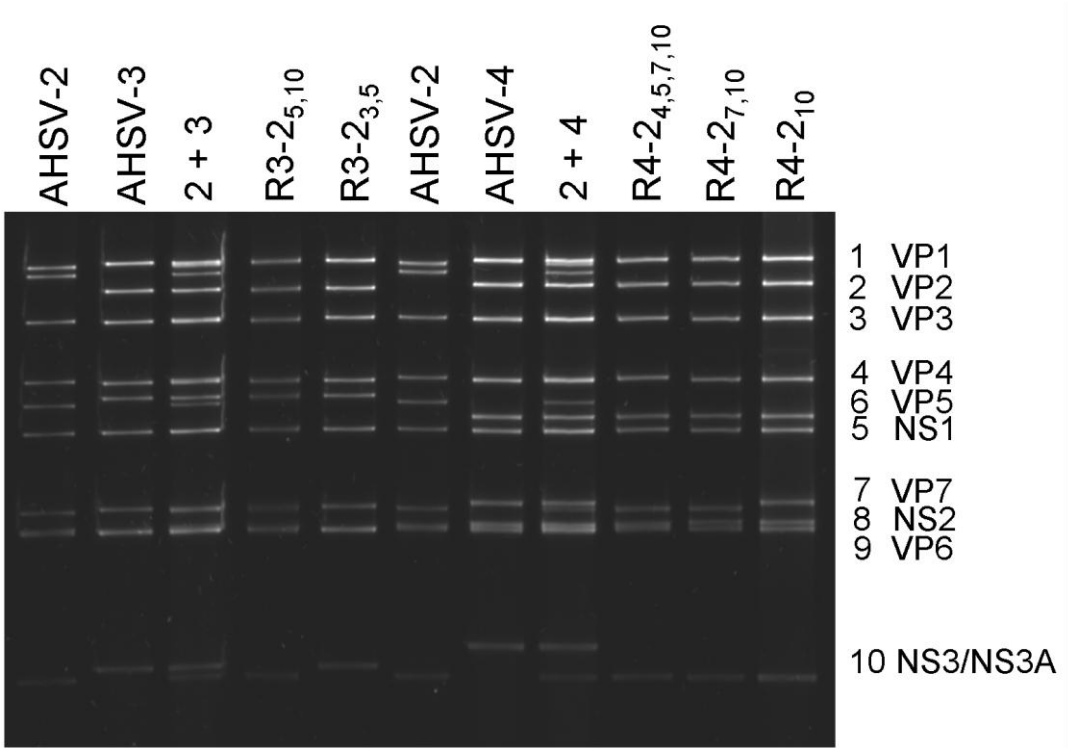

B

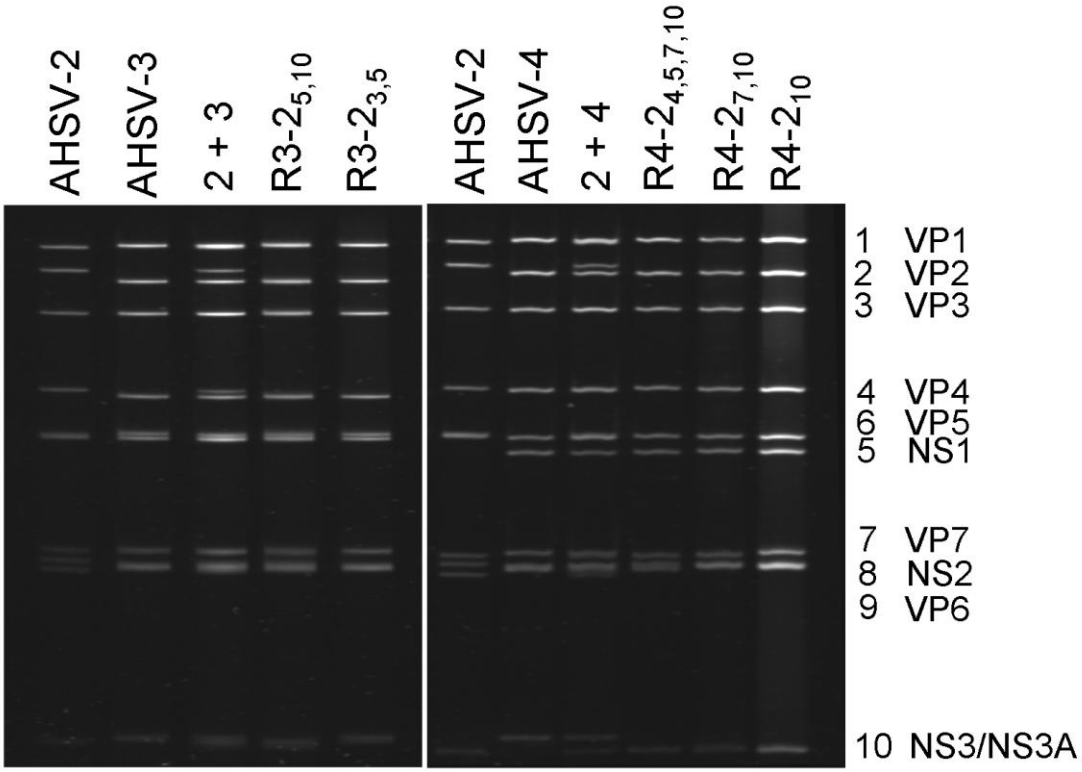

Fig. 2.1 The dsRNA profiles of AHSV-2, AHSV-3, AHSV-4 and reassortant viruses. The dsRNA was isolated from BHK cells infected with the indicated viruses and analysed in a 14% (A) or 6% (B) polyacrylamide gel stained with SYBR gold and visualised under UV illumination. Lanes 3 and 8 were loaded with a mixture of the dsRNA from the respective parental strains. Numbers 1 to 10 on the right indicate the approximate positions of the dsRNA segments; the protein encoded by each segment is also shown. The nomenclature used for the reassortants is described in the text.

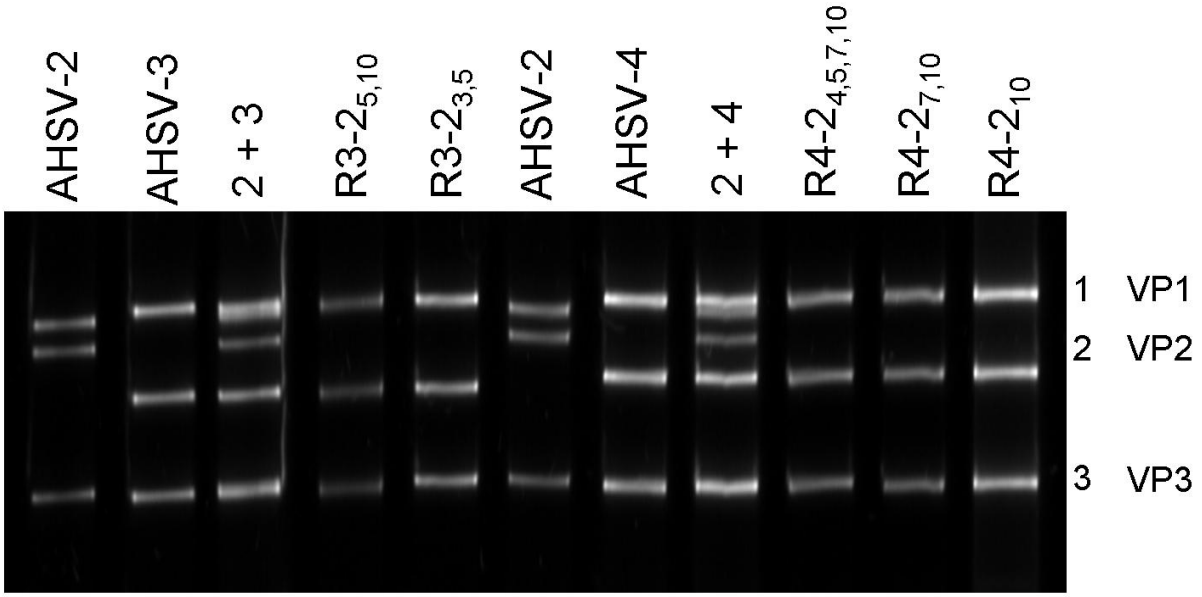

Fig. 2.2 Determination of the parental origin of segment 1 (encoding VP1) of the AHSV reassortants. The dsRNA was analysed on a 14% polyacrylamide gel stained with SYBR gold and visualised under UV transillumination. Lanes 3 and 8 were loaded with a mixture of the dsRNA from the respective parental strains. Numbers 1 to 3 on the right indicate the approximate positions of the dsRNA segments; the protein encoded by each segment is also shown.

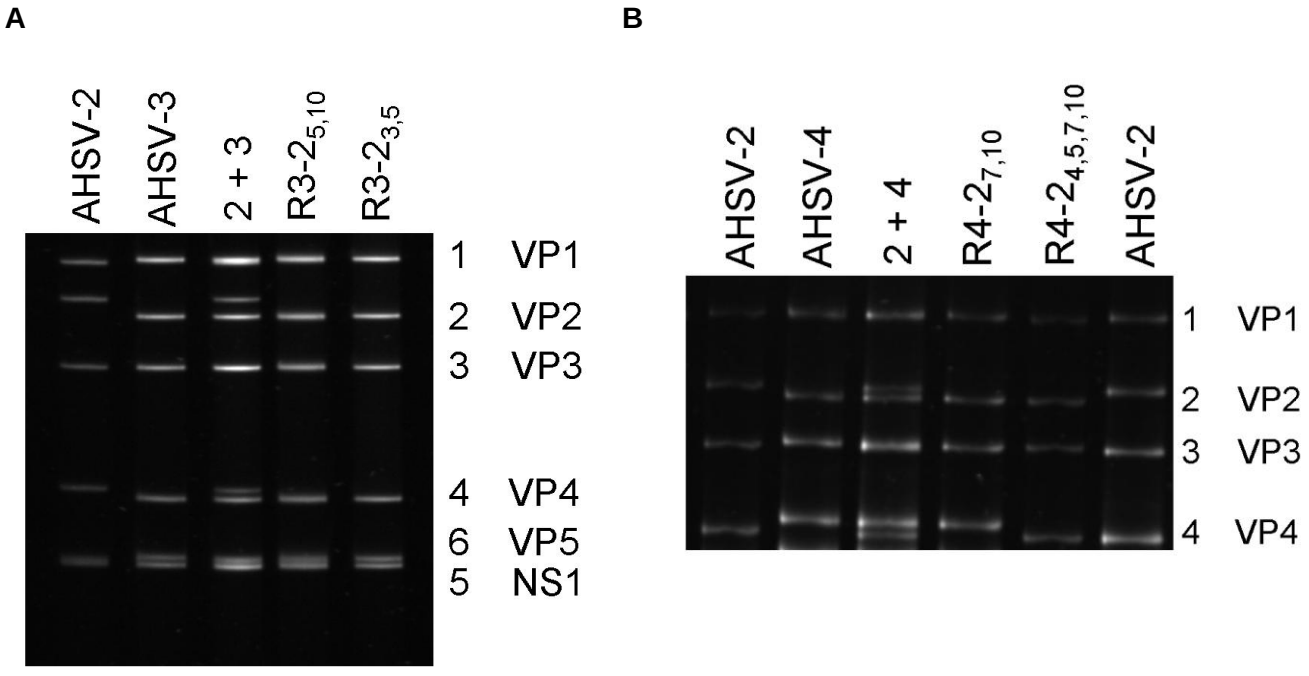

Fig. 2.3 Determination of the parental origin of segment 4 (encoding VP4) of the AHSV reassortants. Viral dsRNA was analysed on a 6% polyacrylamide gel (A) or the PCR products from the amplification of the complete viral cDNA were analysed on an 8% polyacrylamide gel (B) stained with SYBR gold and visualised under UV transillumination. Numbers on the right indicate the approximate positions of the dsRNA or cDNA segments; the protein encoded by each segment is also shown.

For sequencing, the parental and reassortant total dsRNA genomes were converted to cDNA, PCR amplified and the individual genes amplified and sequenced using gene-specific primers. Fig. 2.4 shows the PCR amplification of the genes of reassortant R4-$2_{4,5,7,10}$. Sequences for segments 2, 3, 5, 6, 7, 8, 9 and 10 were aligned and are given in Appendix A.

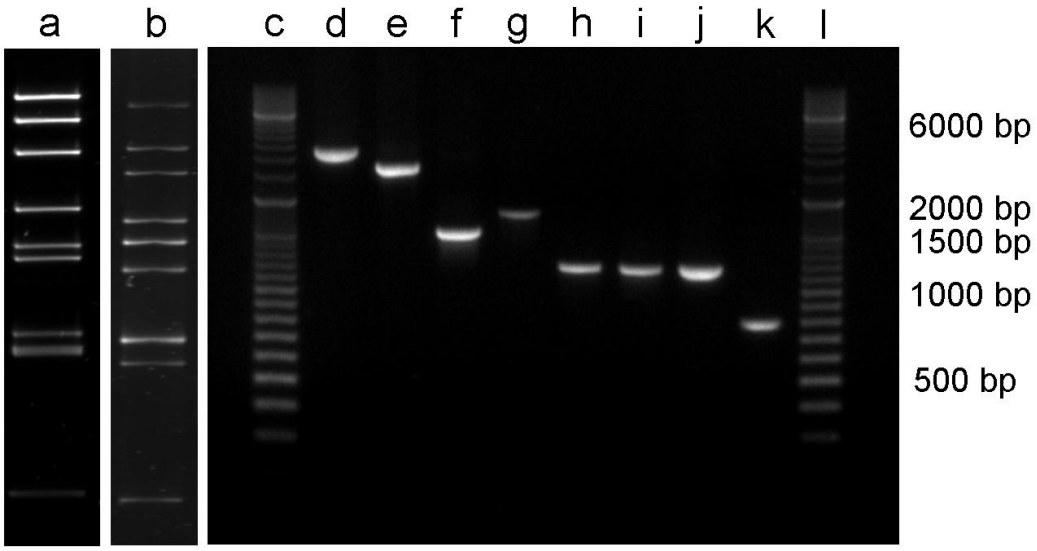

Fig. 2.4 PCR amplification of genes of R4-$2_{4,5,7,10}$ for sequencing. Total viral dsRNA (a) was converted to cDNA using a single-primer amplification sequence-independent method and PCR amplified (b). The genes encoding VP2 (d), VP3 (e), VP5 (f), NS1 (g), VP7 (h), NS2 (i), VP6 (j) and NS3 (k) were then amplified using the gene specific primers listed in Table 2.1. PCR products (d – k) were analysed by 0.8% agarose gel electrophoresis, stained with ethidium bromide (EtBr) and visualised under an UV illuminator. DNA size markers were included in lanes (c) and (l).

The parental origin of the genome segments of the reassortants is summarised in Table 2.3. The nomenclature used for the reassortant viruses (R) is as follows: the first number indicates the parent virus contributing the majority of segments, the second number indicates the parent virus from which the reassorted segments (in subscript) derives. Of the five reassortants that were identified four had the S10 genome segment exchanged. One was a monoreassortant with nine genome segments from AHSV-4 and the S10 genome segment encoding NS3 from AHSV-2 (R4-2_{10}). In addition to S10 the other reassortant viruses had segment 5 encoding NS1 (R3-$2_{5,10}$) or segment 7 encoding VP7 (R4-$2_{7,10}$) or segments 4, 5 and 7 encoding VP4, NS1 and VP7 respectively (R4-$2_{4,5,7,10}$) from AHSV-2. The reassortant R3-$2_{3,5}$ carried segments 3 and 5, encoding VP3 and NS1 respectively, from AHSV-2 in a genetic background of AHSV-3.

Table 2.3 Parental origin of the genome segments of the AHSV reassortants

Segment	Protein encoded	R3-$2_{5,10}$	R3-$2_{3,5}$	R4-$2_{4,5,7,10}$	R4-$2_{7,10}$	R4-2_{10}
1	VP1	3*	3	4	4	4
2	VP2	3	3	4	4	4
3	VP3	3	**2**	4	4	4
4	VP4	3	3	**2**	4	4
5	NS1	**2**	**2**	**2**	4	4
6	VP5	3	3	4	4	4
7	VP7	3	3	**2**	**2**	4
8	NS2	3	3	4	4	4
9	VP6	3	3	4	4	4
10	NS3	**2**	3	**2**	**2**	**2**

* The numbers 2, 3 and 4 in the five columns on the right indicate the parental strains AHSV-2, AHSV-3 and AHSV-4 respectively

No reassortants were identified where the majority of segments originated from AHSV-2 and S10 was contributed by AHSV-3 or AHSV-4. The reason for this phenomenon is not understood but several studies of co-infections with BTV report a similar under-representation of one of the parents, and segments from this parent, among progeny from mixed infections (Ramig *et al.*, 1989). Previous studies of AHSV and BTV reassortants have also shown that non-random segregation of S10 occurs, where the S10 is preferentially derived from one of the parents and may have a selective advantage (Ramig *et al.*, 1989; O'Hara *et al.*, 1998). Co-infections with the parental strains AHSV-3 and AHSV-4 were additionally performed but analysis of 30 progeny plaques revealed no reassortment of S10, indicating that there may be some constraints on the reassortment of the S10 genome segment between these viruses.

2.3.2. Virus yield and release

AHSV particles in both the cellular fractions and medium of infected Vero cells were titrated, and the values combined to represent the total virus yield (Fig. 2.5A) at 24 and 48 h p.i.. The three parental strains AHSV-2, AHSV-3 and AHSV-4 produced similar levels of total progeny virus of between 0.7 - 1.1 x 10^7 pfu/ml. This was important to establish, as it indicates that any phenotypic variations observed between these viruses was not a result of differences in the efficiency of virus production of the strains in Vero cells. Reassortant strains produced high levels of infectious virus, indicating that the exchange of the genome segments in these viruses did not

affect their ability to infect and replicate in Vero cells. Interestingly, reassortants R4-2_{10} and R4-$2_{7,10}$ with a background of AHSV-4 segments containing respectively the NS3 gene or a combination of both the NS3 and VP7 genes from AHSV-2 had titres of up to ten-fold higher than those of AHSV-2 or AHSV-4. Reassortant R4-$2_{4,5,7,10}$, which apart from the NS3 and VP7 genes of AHSV-2 also included the AHSV-2 NS1 and VP4 genes produced titres five-fold higher than those of AHSV-2 or AHSV-4. Reassortants with a background of AHSV-3 segments (R3-$2_{3,5}$ and R3-$2_{5,10}$) were much less affected by reassorting with AHSV-2 genes, showing a two-fold increase in titre over the parental serotype 2 and 3 strains.

As AHSV NS3 has been reported to play a role in virus release (Martin *et al.*, 1998), the relative levels of released virus in parental and reassortant strains was compared. Virus release was calculated by expressing the titres obtained from the culture medium as a percentage of the total titre. The results are shown in Fig. 2.5B**.** The largest proportion of the virus remained cell-associated in all cases, as typically observed with orbiviruses (Eaton *et al.*, 1990). A statistically significantly higher percentage of viruses were released from AHSV-2 infected Vero cells when compared to either AHSV-3 or AHSV-4 infected cells. For example, 32±0.9% of AHSV-2 was extracellular at 24 h p.i compared to 14±2.6% for AHSV-3 ($P < 0.001$) and 21±1.0% for AHSV-4 ($P < 0.001$). The levels of release of the reassortant viruses were similar to that of the parental strain from which their S10 genome segment was derived. Reassortants with S10 from AHSV-2 in a genetic background of either AHSV-3 (R3-$2_{5,10}$) or AHSV-4 (R4-$2_{4,5,7,10}$, R4-$2_{7,10}$ and R4-2_{10}) showed between 35 and 40% release of the total virus produced at 48 h p.i., which is closer to the levels observed for AHSV-2 (39±2.1%) than to either AHSV-3 (20±4.2%) or AHSV-4 (31±3.7%). At the same time point only 22±2.9% of reassortant R3-$2_{3,5}$ was released into the culture medium, which is similar to the AHSV-3 parental strain (20±4.2%, $P = 0.48$) from which the S10 segment derives and significantly different ($P = 0.0002$) from AHSV-2. The presence of the other reassorted segments 3, 4, 5 and 7 did not affect the amount of virus released. Therefore genome segment S10, encoding NS3, appears to be a major determinant in controlling the differences in the percentage virus released between AHSV-2, AHSV-3 and AHSV-4.

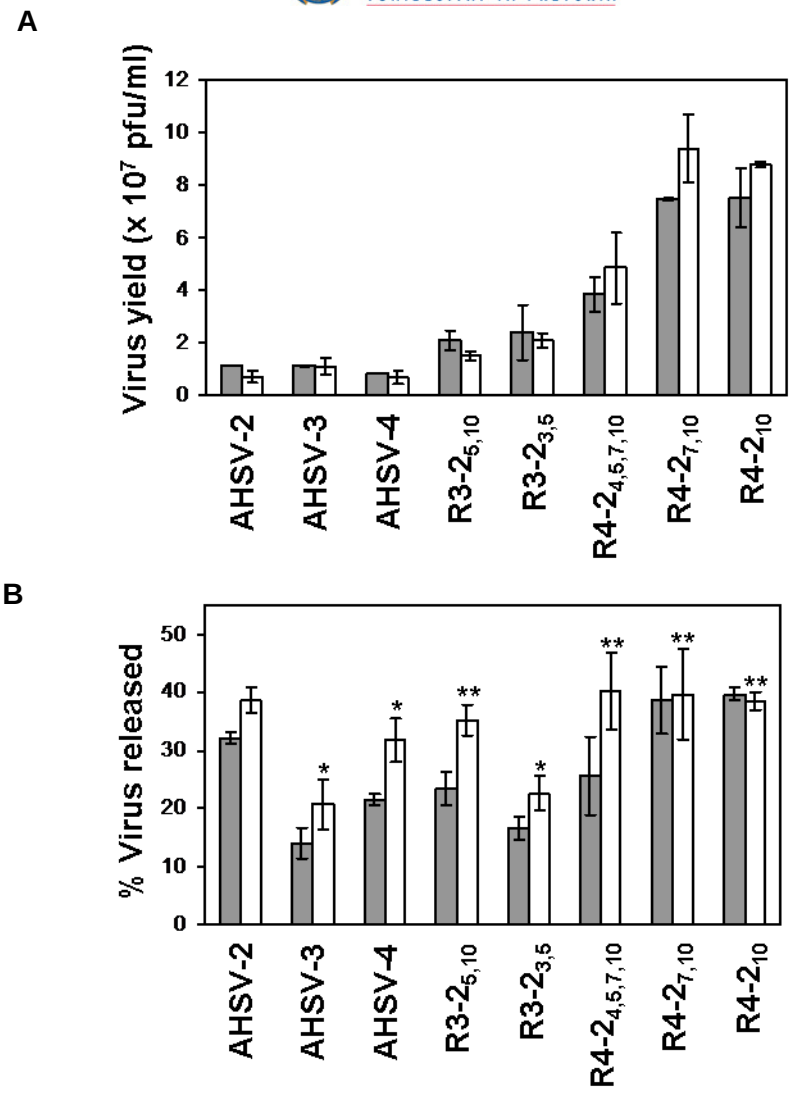

Fig. 2.5 Total infectious virus yield (A) and percentage virus released (B) of parental and reassortant viruses in Vero cells. Cells were infected with the indicated viruses at a MOI of 10 and cell-associated and released virus titrated at 24 h post infection (p.i.; grey columns) and 48 h p.i. (white columns). Values indicate the mean ±SD of two independent experiments with two repeats during each experiment. Values for the parental and reassortant viruses were compared to AHSV-2 by *t* test where * indicates statistically significant difference ($P < 0.01$) and ** indicates no statistically significant difference ($P > 0.05$).

2.3.3. Induction of CPE

The timing and severity of virally induced CPE was scored (Table 2.4) by observing changes in cell morphology, such as shrinking and rounding of cells, loss of contact between neighbouring cells and detachment from the culture plate. The results given in Fig. 2.6 illustrate the effects of the viruses on cell cultures at 48 h p.i. In the case of AHSV-2 CPE was observed at relatively early times post infection (24 h p.i., Table 2.4) with very few cells still attached to the cell culture plate at 48 h p.i. (Fig. 2.6). The development of CPE in AHSV-4 infected cells was a distinctly later event (36 h p.i., Table 2.4) with more cells remaining attached at 48 h p.i. (Fig. 2.6). AHSV-3 infected cells displayed an intermediate phenotype between these two viruses in terms of the

timing of onset of CPE (Table 2.4) but at late times post infection the induced CPE observed was closer to AHSV-2 than AHSV-4 (Fig. 2.6). The CPE of reassortant viruses R3-$2_{3,5}$, R4-$2_{7,10}$ and R4-2_{10} was less than either of the respective parental strains. Of these the monoreassortant R4-2_{10}, with just the NS3 gene of AHSV-2 in the AHSV-4 background, displayed no discernible CPE up to nearly 48h p.i.. In contrast to this, both the timing and severity of the CPE in cells infected with R3-$2_{5,10}$ and R4-$2_{4,5,7,10}$ was closer to that observed for AHSV-2 infected cells than AHSV-3 and AHSV-4 respectively. Based on these observations it can be postulated that simultaneously exchanging both segments 5 and 10 (encoding NS1 and NS3) confers the CPE characteristic of the parent contributing these segments (in this case AHSV-2), while an exchange of only one of the two segments results in reduced CPE. Additional reassortants are, however, required to confirm this.

Table 2.4 Cytopathic effect of AHSV strains on Vero cells infected at a MOI of 5 pfu/cell

Virus Strain	12 h	24 h	36 h	48 h
AHSV-2	-	++	+++	++++
AHSV-3	-	+	++	++++
AHSV-4	-	-	+	+++
R3-$2_{5,10}$	-	++	+++	++++
R3-$2_{3,5}$	-	+	+	+++
R4-$2_{4,5,7,10}$	-	+	+	++++
R4-$2_{7,10}$	-	-	+	++
R4-2_{10}	-	-	-	+

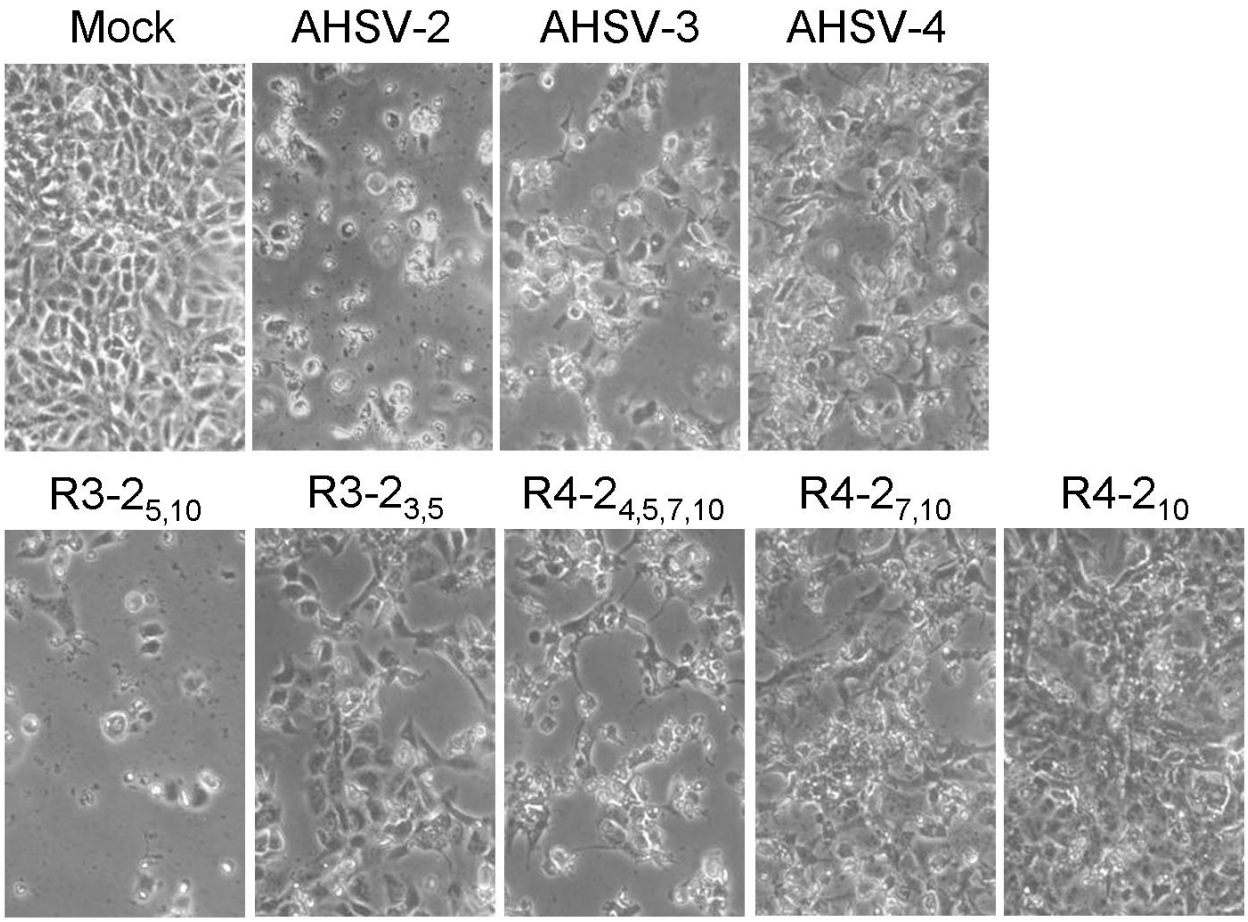

Fig. 2.6 Cytopathic effect of AHSV parental and reassortant strains on Vero cells. Cells were examined 48 h post infection with the indicated viruses (MOI 5 pfu/cell) under a phase contrast microscope.

2.3.4. Infected Vero cell viability and protein synthesis levels

As estimating CPE can be subjective, an additional quantitative measure of cell viability was obtained using the CellTiter-Blue™ cell viability assay (Promega). The results are shown in Fig. 2.7A. AHSV-2 induced rapid cell death, with only 51±1.1% viable cells remaining at 24 h p.i. compared to AHSV-3 (81±3.6%, $P < 0.01$) and AHSV-4 (93±1.2%, $P < 0.01$), these values declined further resulting in 15±0.5%, 22±4.4% ($P < 0.01$) and 36±4.9% ($P < 0.01$) cell viability respectively at 48 h p.i.. All the reassortants, except R4-2_{10}, displayed an intermediate phenotype between the respective parental strains. R4-2_{10} did not induce significant cell death, with 85±2.5% viable cells still remaining at 48 h p.i., which corresponded to the lack of CPE previously observed (Fig. 2.6). There was no clear link between the phenotypes of reassortant viruses and the origin of their NS3 proteins.

As an additional measure of the metabolic activity of infected cells, pulse-labelling with [^{35}S]-methionine was used to monitor total intracellular protein synthesis over an 18 h period as compared to uninfected cells (Fig. 2.7B), before cells started showing distinct CPE. Protein synthesis in AHSV-2 and AHSV-3 infected cells declined rapidly to 34.9±0.72% and 37.4±6.2% respectively of the uninfected control at 18 h p.i. In AHSV-4 infected cells protein synthesis fluctuated closer to that in uninfected Vero cells, at levels of 76.8±2.3% of the control. The values for four of the five reassortants were intermediary to those of the two parental strains. Protein synthesis levels in cells infected with R3-$2_{5,10}$ and R3-$2_{3,5}$ decreased to 35.8±0.12% and 37.9±3.4% compared to the control, and for R4-$2_{4,5,7,10}$ and R4-$2_{7,10}$ the corresponding values were 54.5±2.4% and 65±12.3%. Only in the case of R4-2_{10} did the exchange of the single segment apparently have no effect, resulting in a profile very similar to AHSV-4 with an endpoint value of 83.3±8.8% protein synthesis. Significant correlation was found between the percentage viable cells and percentage protein synthesis ($r = 0.76$, $p = 0.028$). For each of the AHSV strains the decrease in protein synthesis in the period up to 18 h p.i. (Fig. 2.7B) corresponded to the observed subsequent decrease in cell viability as measured by the CellTiter-Blue™ cell viability assay (Fig. 2.7A).

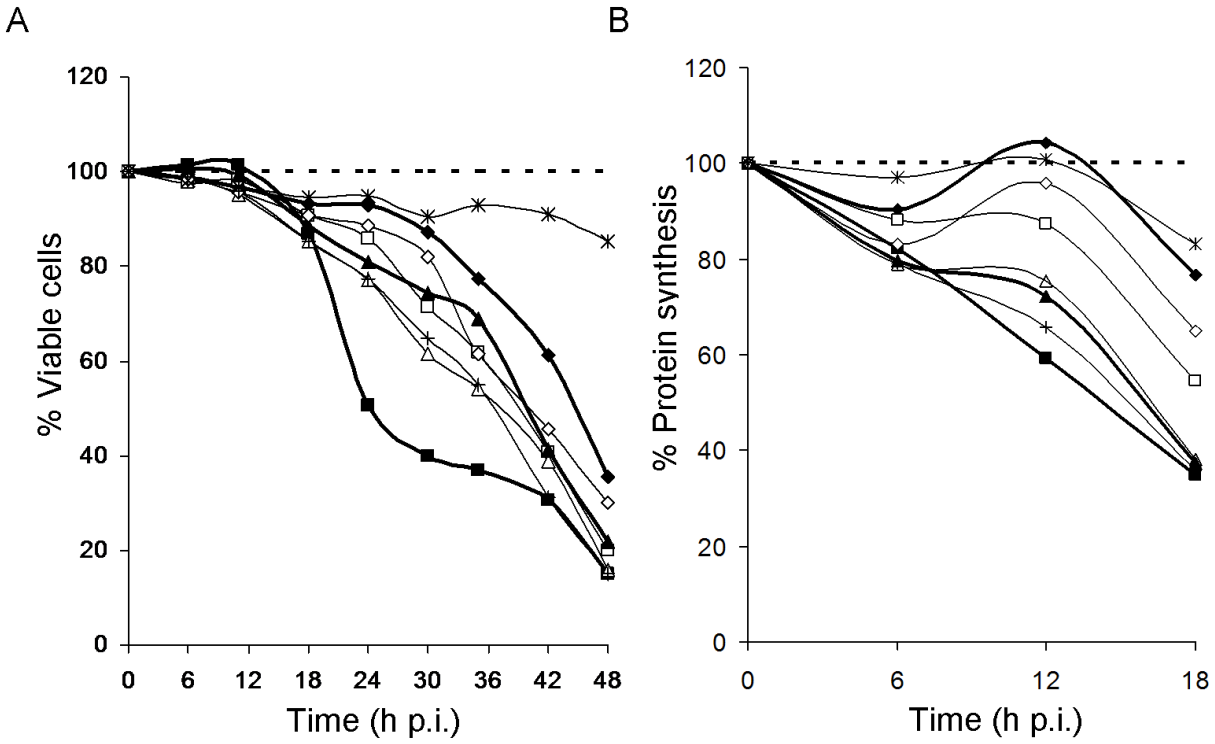

Fig. 2.7 Effect of parental and reassortant AHSV strains on cell viability (A) and total protein synthesis (B) in Vero cells. Cells were infected at a MOI of 10 pfu/cell with AHSV-2 (■), AHSV-3 (▲), AHSV-4 (◆), R3-$2_{5,10}$ (+), R3-$2_{3,5}$ (△), R4-$2_{4,5,7,10}$ (□), R4-$2_{7,10}$ (◇) and R4-2_{10} (✳). Viability was determined over a 48 h period using the CellTiter-Blue™ assay, and protein synthesis monitored by [^{35}S] L-methionine incorporation during a 30 min pulse at 6-hourly intervals up to 18 h p.i. The results in both cases are plotted as a percentage of mock-infected control cells (dashed line). Values indicate the mean of three independent experiments with three repeats during each experiment.

2.3.5. Membrane permeability of infected cells

A Hygromycin B (Hyg B) assay was used to monitor membrane permeability of infected cells. Hygromycin B is a protein synthesis inhibitor that can only penetrate and function in cells after the cell membrane has been permeabilised. Protein translation levels in infected cells, in the presence and absence of Hyg B, is monitored by the measurement of [^{35}S] L-methionine incorporation, see 2.2.6. Decreased levels of [^{35}S] L-methionine incorporation in the presence of Hyg B, in relation to that in the absence of Hyg B, would then indicate permeability of the membrane to Hyg B. The percentage permeabilised cells was calculated as described in 2.2.6. and the results are shown in Table 2.5. Vero cells infected with AHSV-2 consistently showed significantly higher levels of permeabilisation with 67.08±3.32% permeabilised cells compared to AHSV-3 (54.47±5.93%, $P < 0.05$) and AHSV-4 (3.67±3.32%, $P < 0.01$) at 24 h p.i. Cells infected with R4-$2_{4,5,7,10}$, R4-$2_{7,10}$, R4-2_{10} and R3-$2_{5,10}$ were permeabilised to a greater extent than those infected with AHSV-4 or -3 and were closer to that observed for infection with AHSV-2. For example, 67.39±4.33% of the cells infected with R3-$2_{5,10}$ were permeabilised which is significantly closer to the permeabilisation levels of AHSV-2 infected cells ($P = 0.93$) than AHSV-3 infected

cells (P = 0.038). Infection with R3-$2_{3,5}$, the only reassortant that does not contain S10 from AHSV-2, resulted in 54.7±1.38% permeabilisation. This is significantly closer to the effect of AHSV-3 (P = 0.95) than AHSV-2 (P < 0.01). Reassortant viruses therefore showed a tendency towards the levels of permeabilisation observed for the parental virus from which the S10 genome segment was derived. The percentage permeabilised cells was found not to correlate significantly to the percentage viable cells (r = -0.22, p = 0.54) or to the percentage virus released (r = 0.46, p = 0.25). A possible functional link can however not be excluded as sample sizes are relatively small.

Table 2.5 Membrane permeabilisation of Vero cells 24 h after infection with AHSV strains

Virus Strain	% permeabilised cells*
AHSV-2	67.08±3.32
AHSV-3	54.47±5.93
AHSV-4	3.67±3.32
R3-$2_{5,10}$	67.39±4.33
R3-$2_{3,5}$	54.7±1.38
R4-$2_{4,5,7,10}$	80.22±1.10
R4-$2_{7,10}$	76.57±1.35
R4-2_{10}	71.12±1.12

* Values represent mean (n = 3) ± SD

2.4. DISCUSSION

AHSV NS3 is the second most variable AHSV protein, with only outer capsid protein VP2 displaying more variation across all serotypes (Van Niekerk *et al.*, 2001b). This distinguishes it from the highly conserved cognate BTV NS3. The reason for this high level of variation and its impact are not yet clear. In this study three strains of AHSV were selected that each expressed a NS3 protein from one of the three phylogenetic groups, i.e. AHSV-2 (γ NS3), AHSV-3 (β NS3) and AHSV-4 (α NS3). The phenotypic effects of these viruses in mammalian cells was characterised and it was investigated whether this could be linked to the respective NS3 proteins.

Infection with AHSV-2 resulted in significantly higher amounts of membrane permeabilisation, virus release, cell death, morphological damage and cell detachment. AHSV-4 scored lowest in all of these traits and AHSV-3 displayed an intermediate phenotype (closer to AHSV-2). We hypothesised that, firstly, differences in the levels of membrane permeabilisation induced by these viruses could be linked to differences in the encoded α, β, or γ NS3 proteins, based on the finding that recombinant expression of NS3 is cytotoxic to cells possibly as a result of increased

membrane permeabilisation. Secondly, we postulated that in cells infected with AHSV-2, for example, the rapid cell death, high CPE and high amounts of virus release could be linked to the high levels of cell membrane permeabilisation leading to cell lysis. The converse argument would then be true for AHSV-4. As an initial investigation we randomly generated five reassortant viruses selecting for the exchange of the genome segment encoding NS3 to determine the effect on viral phenotype.

The incorporation of AHSV-2 NS3 into a genetic background of AHSV-3 or -4 resulted in an increase in both membrane permeability and the amount of virus released, matching or exceeding that of AHSV-2. These results suggest that the NS3 protein may be the primary determinant of two aspects in the viral life cycle: the amount of virus released from infected cells, and the degree of membrane permeabilisation. This finding confirms previous studies that have shown that the origin of the S10 gene, i.e. whether it groups into the α, β or γ clade, could contribute to the release characteristics of the virus (Martin *et al.*, 1998). Whether the percentage virus released is the direct result of the change in membrane permeability is not yet clear. AHSV and BTV can be released from infected cells either by budding, whereby a temporary lipid envelope is acquired, or by extrusion through a locally disrupted membrane (Eaton *et al.*, 1990; Stoltz *et al.*, 1996). The budding of BTV enveloped particles could result from the interaction of NS3 with components of the vacuolar sorting pathway. This may be the predominant mechanism in insect cells where no CPE is observed (Wirblich *et al.*, 2006). The viroporin activity of NS3 (Han & Harty, 2004) on the other hand could contribute to particle release due to cell lysis, which could be more important in mammalian cells (Wirblich *et al.*, 2006). An interesting preliminary observation (results not shown) was that in KC cells (a *Culicoides* cell line) the trend with respect to virus release was reversed. AHSV-4 displayed the highest percentage release (72.5%), followed by AHSV-3 (43.5%) and then AHSV-2 (35.6%) at 48 h p.i. This emphasises the important contribution of the host cells environment, e.g. proteins and membranes, on the viral release mechanisms.

Membrane permeabilisation, often mediated by a single viral protein or viroporin, can play numerous functions in the viral life cycle and have several consequences for the infected cell. The disorganisation of the cell membrane can facilitate virus budding (Carrasco, 1995; Gonzalez & Carrasco, 2003). Increased permeability to ions and low-molecular-weight compounds also changes the cellular homeostasis of the cell, often promoting viral protein synthesis and providing an ideal environment for virion assembly. Viroporins have furthermore been implicated in the development of CPE by membrane disorganisation and subsequent cell lysis and/or apoptosis (Carrasco, 1995; Gonzalez & Carrasco, 2003; Madan *et al.*, 2008).

Investigation of other aspects, such as cell viability and the development of CPE, showed that these could not be linked to NS3 alone. The incorporation of the NS3 from AHSV-2 into a genetic

background of AHSV-4 in the monoreassortant R4-2_{10}, for example, showed a dramatic increase in membrane permeability and virus release but little to no cell death and CPE. In terms of AHSV cytopathology our results suggest involvement of the non-structural protein NS1, encoded by segment 5, in conjunction with NS3. NS1 is expressed to high levels in infected cells where it forms characteristic tubules, with as yet unknown function. Reassortant viruses with a combination of segments 5 and 10 from AHSV-2 (R3-$2_{5,10}$ and R4-$2_{4,5,7,10}$) displayed a greater tendency towards the AHSV-2 phenotype, with severe CPE. However reassortants in which either AHSV-2 segment 5 (R3-$2_{3,5}$) or 10 (R4-$2_{7,10}$ and R4-2_{10}) were exchanged showed less CPE. In the case of BTV it has been proposed that NS1 is a major determinant of pathogenesis in the vertebrate host, and that modifying the ratio of NS1 to NS3 can shift the mechanism of viral release from a lytic process to one of non-lytic budding from the cell surface (Owens *et al.,* 2004). NS1 tubule formation in BTV-infected mammalian cells was abrogated by the expression of a monoclonal antibody specific to the C-terminal region of NS1 that is essential for tubule formation. This resulted in an increase in the amount of virus released, a shift from lytic release to budding and a dramatic decrease in cellular pathogenesis in these cells. NS1 tubules are found in abundance in BTV-infected insect cells yet there is little CPE in these cells and virus is released by budding. The authors therefore proposed that BTV cellular pathogenesis and release from cells may be a function of the relative ratios of NS1 to NS3 protein levels. In BTV-infected insect cells the levels of NS3 are high in comparison to NS1 so NS3-mediated non-lytic release may allow for the budding of virus without CPE. In mammalian cells, where NS3 levels are lower, NS1 increases virus retention in the cytoplasm, leading to cytolysis and cell death (Owens *et al.*, 2004). The results presented here corroborate the notion that a specific combination of NS1 and NS3 determines AHSV cytopathogenesis, although further investigation is required.

Increased membrane permeability could not, under the conditions used here, be related to increased cell death as proposed for some viroporins. Cell death following viral infection is the endpoint result of a complex interaction of multiple viral and host factors. It is currently unknown whether AHSV induces apoptosis, for example. Recent studies have shown that BTV induces apoptosis in both primary and continuous endothelial cell lines (DeMaula *et al.*, 2001; DeMaula *et al.*, 2002) and that apoptosis is triggered by the outer capsid VP2 and VP5 proteins (Mortola *et al.*, 2004). The mechanism of BTV-induced apoptosis occurs via both caspase-dependant extrinsic and intrinsic pathways (Nagaleekar *et al.*, 2007). Interestingly, BTV induces apoptosis in mammalian cells characterised by extensive CPE but not in insect cells that show no CPE (Mortola *et al.*, 2004). Several viroporins have also been shown to induce apoptosis (Madan *et al.*, 2008). Virus-induced apoptosis may therefore play a significant role in cytopathology.

Our investigation into the amount of infectious virus produced by the reassorted viruses gave surprising results, with an up to ten-fold increase in yield over the parental strains. This increase

in yield may be the result of a combination of factors including the decreased cytopathic effect of some of the reassorted viruses, which would allow for the sustained production of virus, and the increased membrane permeability, which alters the infected cell homeostasis. It would be interesting to investigate whether changes in cell membrane permeability induced by NS3 affects virus replication, protein synthesis and/or assembly. Some viroporins are not essential for viral progeny formation but their expression has been found to significantly increase the production of virus particles (Carrasco, 1995; Gonzalez & Carrasco, 2003; Madan *et al.*, 2008).

In summary, it was shown that non-structural protein NS3 can act in the AHSV life cycle as a viroporin by altering membrane permeability and facilitating virus release from infected cells. The extent of this however depends on which variant of NS3 (α, β, or γ) is carried by the specific virus strain or reassortant. This alteration of membrane permeability by NS3 may fulfil an important function in enhancing virus yield, possibly by altering the infected cell homeostasis. It is clear that NS3 is not the sole determinant of the cytopathic properties of the virus and other viral factors remain under investigation. The NS3 amino acid sequence variation between the isolates used in this study was 34.7% between AHSV-2 and AHSV-3 and 35.2% between AHSV-2 and AHSV-4. This high level of diversity makes it impossible to identify specific residues responsible for the observed phenotypic effects.

In chapter 3 the AHSV-2 NS3 protein was recombinantly expressed in bacterial cells. The cytolytic and membrane permeabilising activity of this protein in these cells was examined, and compared to that of the cognate proteins of BTV and EEV. The regions of AHSV-2 NS3 critical to its cytolytic and membrane permeabilising activity were also examined. In chapter 4 the NS3 proteins from AHSV-2, AHSV-3 and AHSV-4 were recombinantly expressed in insect cells and their exogenous effect on Vero cell membrane permeability compared, in the absence of other AHSV proteins. The cytotoxicity, membrane association and localisation of these proteins expressed in insect cells were also compared in chapter 4.